



SCHOOL OF COMPUTING,  
ENGINEERING AND INFORMATION  
SCIENCES

**Masters Programme in Computing**  
***CG0174 Dissertation***

Student Name Nguyen Thi Thuy Duong(08036127)  
Dissertation Title

An extraction of the Region of Interest and a proposed palmprint  
recognition algorithm using Phase-Only Correlation

2010/11

---

Supervisor: Prof. Ahmed Bouridane

Second Marker: Dr. Joe Faith



# Acknowledgements

Firstly, I would like to thank my supervisor - Prof Ahmed Bouridane for all the opportunities and support he gave me. I also would like to thank my project tutor, reviewer TOR, second marker- Dr Joe Faith for the guidance and instructions during project work period. Finally, I would like to thank the course leader- Shelagh Keogh for being always helpful and obliging.

My family, thank you so much for everything,

Nguyen Thi Thuy Duong

# Declaration

I declare the following:

1. that the material contained in this dissertation is the end result of my own work and that due acknowledgement has been given in the bibliography and references to ALL sources be they printed, electronic or personal.
2. the Word Count of this Dissertation is 12,097.
3. that unless this dissertation has been confirmed as confidential, I agree to an entire electronic copy or sections of the dissertation to being placed on Blackboard, if deemed appropriate, to allow future students the opportunity to see examples of past dissertations. I understand that if displayed on Blackboard it would be made available for no longer than five years and that students would be able to print off copies or download. The authorship would remain anonymous.
4. I agree to my dissertation being submitted to a plagiarism detection service, where it will be stored in a database and compared against work submitted from this or any other School or from other institutions using the service. In the event of the service detecting a high degree of similarity between content within the service this will be reported back to my supervisor and second marker, who may decide to undertake further investigation that may ultimately lead to disciplinary actions, should instances of plagiarism be detected.
5. I have read the UNN/CEIS Policy Statement on Ethics in Research and Consultancy and I confirm that ethical issues have been considered, evaluated and appropriately addressed in this research.

**Signature:**

**Date: 04<sup>th</sup> January 2011**

# Abstract

Biometric has recently paid attention for using in commercial application. A palmprint containing the same features like a fingerprint but is expected to be more distinction than the finger print thank to the larger area of the palmprint and additional distinctive features such as principle lines, ridges, minutiae points, singular points and texture. A major approach has been used based on feature, however, the problem is the accuracy of matching is depends on many environmental factors during the acquisition of the image. This project proposes a palmprint recognition algorithm using Phase- Only Correlation. The use of phase components in 2D Discrete Fourier Transform of palmprint images makes possible to achieve high accuracy palmprint recognition and estimation of translational displacement for normalizing the images before matching. The project also modifies the extraction method of the Region of the Interest for images matching accuracy. The experimental evaluation using PolyU database clearly demonstrates an effective matching performance of the proposed algorithm by using a Matlab language designed programme. The results of evaluation is compared to these methods in Zhang's and Kumar's, which use the 2D Gabor filer for recognition palmprint .

# Contents

<b>Acknowledgements .....</b>	<b>2</b>
<b>Declaration.....</b>	<b>3</b>
<b>Abstract .....</b>	<b>4</b>
<b>0 Chapter 0: Introduction .....</b>	<b>9</b>
0.1 Aims.....	9
0.2 Background .....	9
0.3 Work Done and Results .....	10
0.4 The structure of project.....	11
<b>1 Chapter 1: Background .....</b>	<b>13</b>
1.1 What is biometrics?.....	13
1.2 What is a palmprint?.....	13
1.3 What is a low-resolution palmprint image? .....	14
1.4 What is Phase- Only Correlation? .....	14
1.4.1 General approaches for palmprint recognition.....	14
1.4.2 Phase-only correlation .....	16
1.4.3 Improving robustness using 2D DFT .....	17
<b>2 Chapter 2: Phase-Only Correaltion .....</b>	<b>18</b>
2.1 The principles of Phase - Only Correlation? .....	18
2.1.1 Basic POC.....	18
2.1.2 Band-limited Phase-Only Correlation .....	19
2.1.3 How to determine the upper limits K1 and K2 of the effective frequency components in a given image?.....	20
2.2 Estimation of image rotation.....	20
2.3 Estimation of image translation:.....	21
2.4 Property of shift invariance .....	22
<b>3 Chapter 3. Review of some existing palmprint recognition algorithms .....</b>	<b>23</b>
3.1 2D Gabor phase encoding scheme.....	23
3.1.1 Feature extraction and coding .....	23
3.1.2 Palmprint matching.....	24
3.2 Palmprint identification using PalmCodes.....	25
3.2.1 Normalization .....	25

3.2.2	Multichannel filtering.....	26
3.2.3	Extraction of features .....	26
3.2.4	Identification.....	27
3.3	Extraction of region of interest.....	27
3.3.1	Kuma's .....	27
3.3.2	Zhang's.....	28
<b>4</b>	<b>Chapter 4: Principles of DFTs and image processing techniques in palmprint recognition.....</b>	<b>30</b>
4.1	Hanning Window: .....	30
4.2	The 2-D Discrete Fourier Transform and its Inverse.....	30
4.2.1	Periodicity .....	31
4.2.2	The DFTs of the rotated image.....	32
4.2.3	The DFTs of the shifted image.....	34
4.2.4	The display of the image's DFTs .....	35
4.2.5	A Lowpass filter- Gaussian smoothing.....	37
4.2.6	Threshold binary image.....	38
<b>5</b>	<b>Chapter 5: A proposed algorithm of palmprint recognition.....</b>	<b>40</b>
5.1	The preprocessing stage .....	40
5.1.1	<i>Saving computational time: .....</i>	<i>41</i>
5.2	The extraction of ROI.....	41
5.2.1	<i>How can to determine the corners of the area between the ring and middle fingers. 42</i>	
5.3	The matching stage .....	42
<b>6</b>	<b>Chapter 6: Evaluation of results, methods, and aims. ....</b>	<b>44</b>
6.1	Verification and recognition.....	44
6.1.1	Verification: Am I who I claim to be? .....	44
6.1.2	Identification/Recognition: Who am I? .....	44
6.2	FAR, FRR, ROC and EER.....	45
6.2.1	Impostor patterns and FAR.....	45
6.2.2	Client patterns and FRR.....	45
6.2.3	Receiver Operating Characteristic (ROC) .....	46
6.2.4	The equal error rate (EER).....	46
6.3	Evaluation of results .....	47

6.3.1	Verification accuracy .....	47
6.3.2	Identification/Recognition accuracy .....	48
	Figure 6.5: The EER and ROC with threshold = 0.4 .....	49
6.4	Evaluation of methods .....	50
6.4.1	The factors impacting on the accuracy of the image normalizing.....	50
6.5	Evaluation of aims and objectives.....	52
6.5.1	Aims.....	52
6.5.2	Objectives.....	52
<b>7</b>	<b>Chapter 7: Conclusions and Recommendations .....</b>	<b>53</b>
7.1	Conclusions .....	53
7.2	Further work .....	53
	<b>Bibliography .....</b>	<b>55</b>
	<b>Appendix A. Figures and diagrams .....</b>	<b>58</b>
	Figure 1.1 : Palmprint feature definition principal lines and wrinkles.....	58
	Figure 2.1: When two image are similar and dissimilar, comparison between POC and original correlation.....	59
	Figure 2.2: Comparison between POC and BLPOC.....	60
	Figure 3.1: the procedure of PalmCode of Kuma(2004).....	60
	Figure 3.2: Comparison of Extracting ROI between Zhang's and project's .....	61
	Figure 4.1: Hanning Image .....	62
	Figure 4.2: Period of DFT .....	62
	Figure 4.3 Display of DFT.....	63
	Figure 5.1 the centre of gravity of the image. ....	64
	Figure 5.2 Amplitude spectrum.....	64
	Figure 5.3 Log-Polar Mapping Image .....	64
	Figure 5.4 Preprocessing of proposed method .....	65
	Figure 5.5: How to find the place of A and B points.....	66
	Figure 5.6 The Procedure to extract Region of Interest.....	67
	Figure 5.7: Matching stages.....	68
	Figure 6.1: FRR, FAR and Threshold.....	69
	Figure 6.2 A sample of Palmprint image in PolyU database.....	70
	Figure 6.3: Preparation of database.....	71
	<b>Appendix B. Terms of reference .....</b>	<b>72</b>



**Appendix C. Codes.....**Error! Bookmark not defined.

# 0 Chapter 0: Introduction

## 0.1 Aims

The main purpose of this project is to propose an effective algorithm to improve palmprint recognition using Phase-Only Correlation. The aims is identified for this problem consists of determining the area of palmprint and applying some image processing techniques to them (Region of Interest Extraction), modifying Phase-only Correlation to improve palmprint recognition and evaluating the proposed algorithm and compare it to some existing and similar ones.

## 0.2 Background

The rapid growth of e-commerce applications requires reliable and automatic personal identification for effective security access/control. While traditional, automatic, personal identification approaches have some limitations such as a physical key, an ID card, and a passport stolen or lost; a password guessed or forgotten, Biometric personal identification is emerging as a powerful means for automatically recognizing a person's identity.

Among many biometric techniques, palmprint recognition is one of the most reliable approaches, since a palmprint has a large inner surface of the hand containing many features such as principle lines, ridges, minutiae points, singular points and texture. Compared with other biometric traits, the advantages of palmprint are the availability of large palm area for feature extraction, the simplicity of data collection and high user acceptability.

A palmprint image can be analyzed as texture, which is random rather than uniform. Any commercial development of an automated palmprint based identification system would require automated extraction of region of interest - palmprint area, while ignoring fingers, wrist, and background.

A major approach for palmprint recognition today is to extract feature vectors corresponding to individual palmprint images and to perform palmprint matching based on some distance metric. However, one of the most difficult problems of palmprint recognition is that the matching performance is significantly influenced by

many parameters at the feature extraction process, which may vary depending on environmental factors of palmprint image acquisition. The reliability on the performance of a personal recognition system largely depends on its degree of tolerance due to rotation, translation, and scaling distortions.

Fortunately, Phase Only Correlation (POC) has some remarkable properties such as invariance to image translation, invariance to illumination changes, and immunity against additional noise. The technique could be successfully applied to fingerprint recognition, iris recognition and shoeprint recognition already.

### **0.3 Work Done and Results**

The purpose of this project consisted of two largely parts: theory research and practical development. The theory research requires the huge of knowledge of the applied mathematics in the image processing area. Particularly, the research included the principle of 2D- DFTs and Phase-Only Correlation known as the theoretical part of the proposed algorithm. What's more, the author was required to familiar with image processing functions written in Matlab. In order to evaluate the project, the author has been learnt some kinds of typical biometric scenario of a control access point application, including recognition, verification and watch-list.

This project proposed an effective algorithm for palmprint recognition using phase-based image matching in 2D Discrete Fourier Transforms(DFTs) having been effectively applied to fingerprint, shoeprint and iris recognition. It seemed that it were possible to apply the fingerprint recognition method on the palmprint recognition and to improve the calculation of Hanning window, amplitude spectrum and thus log-polar mapping of plamprint as well. The project also extracted successfully the Region of Interest, which was modified from Zhang's method. However, there was no comparison of these methods in term of effectiveness on the accuracy of matching.

The speed of the proposed algorithm was rather slow. The results of project were not better than Zhang's algorithm- a feature-based method in part, although the "EER" parameter equals to 2%. There was not investigation of estimation rotation and translation in preprocessing before matching. Finally, instead of automatic input value, the use of constant input value may affect on the accuracy of the matching in

spite of reduce the computational time and the programming. All of these disadvantages may impact negative on the results of the proposed algorithm.

#### **0.4 The structure of project.**

Chapter 1 introduces the important roles of biometric systems in commercial applications and explains why palmprint is given more attention. A brief discussion of low-resolution palmprint images is presented. Finally, several advantages of phase-based image matching in 2D Discrete Fourier Transforms(DFTs) are shown to support the motivation for choosing this topic.

Chapter 2 discusses the principle of phase-based image matching using the Phase-Only Correlation (POC) function including the basic POC and the band-limited POC. The way how to find upper limits  $K_1$  and  $K_2$  of the effective frequency components in the band-limited POC is given in detail. The estimation of rotation angle and translational displacement is gathered for normalizing the images to improve high accuracy of matching.

Chapter 3 investigates two existing palmprint recognition algorithms using 2D real and complex Gabor phase, which are compared to the proposed method using Phase components in 2D discrete Fourier Transform.

The last section is concerned with with a brief description of existing methods for extracting region of interest using Kuma's method and Zhang's method and identifies the most sufficient technique for modifying the ROI extraction method as the combination of Zhang's and Kuma's.

Chapter 4 presents brief theory basics of image processing techniques in Discrete Fourier Transform, including the periodicity and display of DFTs, and the DFTs of the rotated image, shifted image used for calculating the POC function. What's more, in order to create effectively a ROI- database used for the matching stage in proposed method, three techniques, including a low pass filter, a threshold and a boundary tracking are discussed in the section.

In chapter 5, a palmprint recognition algorithm using Phase-Only correlation is proposed by combining basic ideas from Ito (2003) with the ROI extracting technique of Zhang (2003) and the estimation rotation angle of Takita(2003).

The input of the procedure is a stored palmprint image  $f(n_1, n_2)$  and a palmprint image  $g(n_1, n_2)$  which to be verified.

The output of the procedure is the degree of the similarity.

The basic theory of the algorithm is presented in the previous chapters.

The proposed algorithm consists of the three stages including preprocessing, extraction of ROI and palmprint matching. The Preprocessing stage is used to normalize the images rotation and/or translation (as presented in the section 5.1) are computed and used for alignment purposed. The extraction of Region of interest (ROI) is modified from the method in Zhang's paper, introduced in section 5.2. The palmprint matching stages is used the method in Ito's paper (2006).

Chapter 6 aims to explain how the proposed algorithm is implemented, including evaluations of results, methods, and aims.

In order to evaluate the project, the brief summary of verification and recognition scenarios with standards known as FAR, FRR, EER and ROC is presented at the beginning of the chapter.

Chapter 7 concludes the whole investigation and research carried out. This part highlights issues found during the project period supporting the hypothesis introduced in the previous chapters.

# 1 Chapter 1: Background

This chapter introduces the important roles of biometric systems in commercial applications and explains why palmprint is given more attention. A brief discussion of low-resolution palmprint images is presented. Finally, several advantages of phase-based image matching in 2D Discrete Fourier Transforms(DFTs) are shown to support the motivation for choosing this topic.

## 1.1 What is biometrics?

Current security mechanisms are becoming increasingly deployed in many applications today. For example, reliable and automatic personal identification using human's physiological traits are useful for improved security. Typically, there are two categories of traditional automatic, personal identification including token based and knowledge-based. The token-based one is known as a physical key, and a passport or ID card while knowledge-based one is known as a password. In the token-based application, on the other hand, stealing or losing a passport or a physical key could cause the negative impacts on commercial application. In the knowledge based approach, in addition, a password can be guessed or forgotten. Therefore, in order to avoid these limitations, biometric personal identification is emerging as a powerful means for automatically recognizing a person's identity. Indeed, many biometric systems for commercial applications have been successfully developed, such as fingerprint, palmprint, voice, face, and iris-based verifications have been considered widely (Lee and Gaensslen, 2001; Zhang, 2003; Daugman, 1993; Reillo, Avilla and Gonzalez, 2000; Wildes, 1997; Zhang, 2002).

## 1.2 What is a palmprint?

Over the last 25 years, fingerprint recognition has been paid significant attention. However, it is impossible for workers and the old to supply clear fingerprint due to their problematical skins and physical work. The large inner surface of a hand called a palmprint(Figure 1.1), provides a lot of unique features naming principle lines, minutiae points, singular points and texture regarded more characteristic than a fingerprint in representation(Zhang, 2004; Shu and Zhang, 1998). In addition,

because of dealing with automatically recognizing individual based on their unique palms feature, palmprint biometrics is useful for forensic investigation and commercial applications such as access control (Laadjel, 2009). Nevertheless, studying and researching on palmprint identification and verification has reported limitedly, despite the importance of palmprint features. Palmprint-based personal identification has been known as one of the most trustworthy approaches in biometric techniques (Lee and Gaensslen, 2001; Zhang, 2003; Daugman, 1993; Reillo, Avilla and Gonzalez, 2000; Wildes, 1997; Zhang, 2002).

### **1.3 What is a low-resolution palmprint image?**

Depending on the requirement of applied purposes, images can be used with high or low resolutions. The high resolution palmprints (500 Dpi or higher) are more useful for the requirements of law enforcement such as forensic usage (Dai and Zhou, 2010). For commercial applications, conversely, palmprint recognition generally concentrates on low resolution (about 150 ppi or less) palmprints. In addition, image resolution depend on what kind of features are needed to be extracted. For example, minutiae points, ridges, and singular points are required to extract with a high-resolution image with at least 400 dpi (dots per inch) (Shi et al, 2003). On the other hand, principal lines and wrinkles (Figure 1) are obtained from a low-resolution image with less than 100 dpi (Zhang and Shu, 1999; Shu and Zhang, 1998).

Generally, because of the smaller file sizes, low resolution palmprint images are more suitable than high-resolution ones in civil and commercial applications. They are really useful for a lot of real time application thanks to results in shorter computation times during pre-processing and feature extraction thus requiring low cost sensor and less memory.

### **1.4 What is Phase- Only Correlation?**

#### **1.4.1 General approaches for palmprint recognition**

One of the most important conventional algorithms for palmprint recognition is to use the extraction of feature vectors and the performance of palmprint matching based on some distance metrics (Duta, Jain and Mardia, 2002; Zhang, 2003). During feature extraction process, nevertheless, depending on environmental factors of

image acquisition, many parameters can considerably influence the performance of matching, and thus the high accuracy of matching can be affected negatively. Fortunately, analyzing a palmprint image as texture can be random rather than uniform. Zhang *et al* (2003) proposed a 2D Gabor phase encoding scheme for palmprint feature extraction and representation. In order to represent a low-resolution palmprint image and match different palmprint images, Zhang *et al* (2003) extend 2D Gabor phase coding to represent a palmprint image using its texture feature, and apply a normalized Hamming distance for the matching measurement. The high genuine accept rate (GAR) was achieved with 98 percent and the equal error rate (EER) is 0.6 percent, which had comparison with other hand-based biometrics, such as hand geometry and fingerprint verification (Jain *et al*, 2000; Jain, Hong and Bolle, 1997; Sanchez-Reillo, Avilla and Gonzalez-Marcos, 2000).

However, because of using complex Gabor filter masks of 31x31 sizes, the computational complexity of Zhang's method (2003) is about as twice as that of the algorithm of Kumar (2004). Kumar (2004) investigated a new method for the palmprint identification using Real Gabor Function (RGF) filtering. The computational complexity was reduced mainly thanks to using of RGF mask of size 13x13. However, the palmcode representation used in this method is not rotation invariant (Kumar, 2004). In addition, the accuracy of Kumar's method depends on updating the training database due to physiological growth and small size of available database.

Because a palmprint image can be represented by some line features from a low-resolution image, the stack filter is an effective algorithm to extract the principal lines (Wu and Li, 1997). However, these principal lines are not sufficient to represent the uniqueness of each individual's palmprint due to similar principal lines in different people's palmprints (Zhang, 2003). Additionally, some palmprint images do not have clear wrinkles; Zhang (2003) tried to extract texture features from low-resolution palmprint images.



#### 1.4.2 Phase-only correlation

As mentioned above, a range of approaches for images registration have been developed over the years, for example methods using image-feature-based methods , Fourier- transform-based methods, image correlation functions, image-feature-based methods, and others (Nagashima, 2006; Zhang, 2003; Gueham, 2007). Recently, novel techniques using a phase-only Correlation function has been paid more attention to achieve the high-accuracy registration. The POC- based image registration enables to estimate the displacement between images with subpixel accuracy from the correlation peak location. The most remarkable properties the POC are invariable to image translation, invariance to illumination change, and immunity against additional noise.

In addition, the other benefit of using POC is extended to the rotated, translated, and scaled images matching (Nagashami, 2006). With the use of this matching method, the rotation angle can be converted into image translation. As a result, estimating high-accuracy images translational displacements of images with high accuracy is one of the most important stages in the matching algorithms. Takita(2003) have proposed a high accuracy POC based image matching method that can estimate translational displacement between images with subpixel resolution. The method also employed an analytical function fitting technique, a Hanning windowing technique, and a spectrum weighting technique in order to improve the estimations Takita(2003). Ito(2006) used the method in Takita's paper for his proposed method. (Nagashima, 2006) extended the method to high-accuracy block matching in order to find the corresponding point pairs between two images. Moreover, Gueham, Bouridane and Crookes (2007) combined a spectral weighting function with the POC technique in image registration in order to enhance the registration accuracy of not only palmprint but also shoeprint.

Zhang (2003) used the hand shape for the alignment of different palmprint images obtained for matching, therefore, if the palm-center part is needed to extract, it is requirements of controlling the hand placement by using pegs. Takita(2003) proposed a method employing the high-accuracy image registration approach using Phase-Only Correlation. Ito (2006) also estimated rotation angle and translational

displacement between images by using phase information. As a result, it is possible to develop a palmprint recognition system without controlling the placement of a hand (Ito, 2004; Ito, 2006; Takita, 1003). The project combines the method of extract ROI in Zhang's paper with the method of estimate displacement using Phase-Only Correlation to propose a palmprint recognition algorithm with a high accuracy matching.

#### **1.4.3 Improving robustness using 2D DFT**

The use of phase components in 2D(two-dimensional) discrete Fourier transforms of palmprint images makes it possible to achieve highly robust palmprint recognition(Ito, 2006). The recognition performance of these algorithms is degraded for palmprint images having nonlinear distortion due to hand movement, because these algorithms consider just rigid body transformation among palmprint images. Iitsuka, Ito and Aoki(2008) have presented a effective palmprint recognition algorithm using Phase Only Correlation(POC) which is an image matching technique using the phase components in 2D Discrete Fourier Transforms(DFTs) of given images.

In summary, this project proposes an effective algorithm for palmprint recognition using phase-based image matching in 2D Discrete Fourier Transforms(DFTs) especially that DFT has been been effectively applied to fingerprint, shoeprint and iris recognition(Ito, 2004; Ito, 2005; Nakajima, 2005; Miyazama *et al* , 2005; Gueham, 2007). Normally, there are three stages in a recognition algorithm including Preprocessing, extraction of ROI and matching. In order to extract the centre part of a palmprint for accurate matching, the method described in Zhang's article has been used regularly (Ito, 2008). Therefore, the project will combine the extraction of ROI in Zhang's paper (2003) with the estimation of rotation and translation of the fingerprint images in Ito's paper (2003) and the improved calculation POC techniques in Ito's paper (2006) and Takita 's paper(2003), in which the phase components are in 2D Discrete Fourier Transform.

## 2 Chapter 2: Phase-Only Correlation

This chapter discusses the principles of phase-based image matching using the Phase-Only Correlation (POC) function including the basic POC and the band-limited POC. The way how to find upper limits K1 and K2 of the effective frequency components in the band-limited POC is given. The estimation of rotation angle and translational displacement is gathered for normalizing the images to improve high accuracy of matching.

### 2.1 The principles of Phase - Only Correlation?

#### 2.1.1 Basic POC

Consider two  $N_1 \times N_2$  images,  $f(n_1, n_2)$  and  $g(n_1, n_2)$ , where the index ranges are  $n_1 = -M_1, \dots, M_1$  ( $M_1 > 0$ ) and  $n_2 = -M_2, \dots, M_2$  ( $M_2 > 0$ ) or mathematical simplicity, and hence  $N_1 = 2M_1 + 1$ ,  $N_2 = 2M_2 + 1$ . Let  $F(k_1, k_2)$  and  $G(k_1, k_2)$  denote the 2D DFTs of the two images.  $F(k_1, k_2)$  is given by

$$\begin{aligned} F(k_1, k_2) &= \sum_{n_1, n_2} f(n_1, n_2) W_{N_1}^{k_1 n_1} W_{N_2}^{k_2 n_2} \\ &= A_F(k_1, k_2) e^{-j\theta_F(k_1, k_2)} \end{aligned}$$

Where  $k_1 = -M_1, \dots, M_1$ ,  $k_2 = -M_2, \dots, M_2$ ,  $W_{N_1} = e^{-j\frac{2\pi}{N_1}}$ ,  $W_{N_2} = e^{-j\frac{2\pi}{N_2}}$  and  $\sum_{n_1, n_2}$  denotes  $\sum_{n_1=-M_1}^{M_1} \sum_{n_2=-M_2}^{M_2}$ .  $A_F(k_1, k_2)$  is amplitude and  $\theta_F(k_1, k_2)$  is phase.  $G(k_1, k_2)$  is defined in the same way. The cross-phase spectrum  $R_{FG}(k_1, k_2)$  is given by

$$R_{FG}(k_1, k_2) = \frac{F(k_1, k_2) \overline{G(k_1, k_2)}}{|F(k_1, k_2) \overline{G(k_1, k_2)}|} = e^{j\theta(k_1, k_2)}$$

Where  $\overline{G(k_1, k_2)}$  is the complex conjugate of  $G(k_1, k_2)$  and  $\theta(k_1, k_2)$  denotes the phase difference  $\theta_F(k_1, k_2) - \theta_G(k_1, k_2)$ . The POC function  $r_{fg}(n_1, n_2)$  is the 2D Inverse DFT (2D IDFT) of  $R_{FG}(k_1, k_2)$  and is given by

$$r_{fg}(n_1, n_2) = \frac{1}{N_1 N_2} \sum_{k_1, k_2} R_{FG}(k_1, k_2) W_{N_1}^{-k_1 n_1} W_{N_2}^{-k_2 n_2}$$

Where  $\sum_{k_1 k_2}$  denotes  $\sum_{k_1=-M_1}^{M_1} \sum_{k_2=-M_2}^{M_2}$ . When two images  $(n_1, n_2)$ ,  $g(n_1, n_2)$ , are the same image, i.e.,  $f(n_1, n_2) = g(n_1, n_2)$ , the POC function will be given by

$$\begin{aligned}\hat{r}_{ff}(n_1, n_2) &= \frac{1}{N_1 N_2} \sum_{n_1, n_2} R_{FG}(k_1, k_2) W_{N_1}^{-k_1 n_1} W_{N_2}^{-k_2 n_2} \\ &= \delta(n_1, n_2) \\ &= \begin{cases} 1 & \text{if } n_1 = n_2 = 0 \\ 0 & \text{otherwise} \end{cases}\end{aligned}$$

The above equation implies that the POC function between two identical images is the Kronecker's delta function  $\delta(n_1, n_2)$  (Ito, 2008). The most significant benefit of POC compared to the ordinary correlation is its accuracy in image matching (Ito, 2008).

When two images are similar, their POC function gives a distinct sharp peak.

When two images are not similar, the peak drops significantly. The height of the peak gives a good similarity measure for image matching, and the location of the peak shows the translational displacement. Thus, the POC function exhibits much higher discrimination capability than the ordinary correlation function (Figure 2.1). Other important properties of POC function used for image matching is that it is not influenced by image shift and brightness change, and it is highly robust against (Ito, 2004; Laadjel et al, 2009).

### 2.1.2 Band-limited Phase-Only Correlation

In addition to improvement of POC, Ito (2008) has proposed a BLPOC (Band-limited Phase-Only Correlation) function dedicated to biometric authentication tasks (Figure 2.2). The idea is to eliminate meaningless high frequency components of palmprint images.

Indeed, assume that the ranges of inherent frequency band are given by  $k_1 = -K_1, \dots, K_1$  and  $k_2 = -K_2, \dots, K_2$ , where  $0 \leq K_1 \leq M_1$  and  $0 \leq K_2 \leq M_2$ . Thus the effective size of frequency spectrum is given by  $L_1 = 2K_1 + 1$  and  $L_2 = 2K_2 + 1$ . The BLPOC function is given by

$$r_{fg}^{K_1 K_2}(n_1, n_2) = \frac{1}{L_1 L_2} \sum'_{k_1, k_2} R_{FG}(k_1, k_2) W_{N_1}^{-k_1 n_1} W_{N_2}^{-k_2 n_2}$$

Where  $n_1 = -K_1, \dots, K_1$ ,  $n_2 = -K_2, \dots, K_2$  and  $\sum'_{k_1, k_2}$  denotes  $\sum_{k_1=-K_1}^{K_1} \sum_{k_2=-K_2}^{K_2}$

Ito et al (2006) also noted that the maximum value of the correlation peak of the BLPOC function was always normalized to 1. Because there is not dependent between the maximum peak value and the size of frequency spectrum ( $L_1$  and  $L_2$ ) (Ito et al, 2006). The shape of the band-limited POC function for the two identical images is always the Kronecker's delta function  $\delta(n_1, n_2)$ . Also note that the original POC function can be presented as

$$\hat{r}_{fg}(n_1, n_2) = \hat{r}_{fg}^{M_1 M_2}(n_1, n_2)$$

### 2.1.3 How to determine the upper limits K1 and K2 of the effective frequency components in a given image?

Ito (2004) automatically determined  $K_1$  and  $K_2$  depending on the input image as follows:

- i) Compute the amplitude spectrum of a input image by 2D DFT.
- ii) Compute  $k_2$  - axis projection  $p_{k_2}(k_1)$  and  $k_2$ -axis projection  $p_{k_1}(k_2)$  of the amplitude spectrum.
- iii) Compute the mean values  $\mu_{p_{k_2}}$  and  $\mu_{p_{k_1}}$  for the two projections  $p_{k_2}(k_1)$  and  $p_{k_1}(k_2)$ , respectively.
- iv) Define the parameters  $K_1$  and  $K_2$  as

$$K_1 = \max \left( \left\{ k_1 \mid p_{k_2}(k_1) \geq \mu_{p_{k_2}}, 0 \leq K_1 \leq M_1 \right\} \right),$$

$$K_2 = \max \left( \left\{ k_2 \mid p_{k_1}(k_2) \geq \mu_{p_{k_1}}, 0 \leq K_2 \leq M_2 \right\} \right)$$

Note that the amplitude spectrum is even symmetric for every axis.

Practically, the parameter of the BLPOC function is  $K_1/M_1 = K_2/M_2 = 0.5$ . It is useful to eliminate the meaningless high frequency components and reduce the size of phase information based on the symmetry property of DFT and quantization (Ito, 2008). The upper half of the phase components is eliminated.

## 2.2 Estimation of image rotation

The POC function is sensitive to the image rotation, and it is necessary that to normalize the rotation angle between the registered image  $f(n_1, n_2)$  and the input image  $g(n_1, n_2)$  in order to perform the high accuracy matching. Ito(2004) proposed a straightforward method of estimation of rotation between fingerprint images. The project will apply this idea to estimate the angle rotation between palmprint images.

Ito(2004) performed the rotation alignments less than  $\pm 1$  degree for high accuracy fingerprint matching using the POC function. Firstly, a set rotated images  $f_{\theta}(n_1, n_2)$  of the registered fingerprint  $f(n_1, n_2)$  over the angular range  $-\theta_{max} \leq \theta \leq \theta_{max}$  with an angle space 1 degree. Ito(2004) use  $\theta_{max} = 20$  degree in the experiment. The rotation angle  $\theta$  of the input is determined by evaluating the similarity between the registered image  $f_{\theta}(n_1, n_2)$  ( $-\theta_{max} \leq \theta \leq \theta_{max}$ ) and the input image  $g(n_1, n_2)$  using POC function.

### 2.3 Estimation of image translation:

The translational displacement is aligned between the rotation-normalized image  $f_{\theta}(n_1, n_2)$  and the input image  $g(n_1, n_2)$ . The displacement can be obtained as the peak location of the POC function between  $f_{\theta}(n_1, n_2)$  and  $g(n_1, n_2)$ . Takita(2003) estimates the displacements calculating the log-polar mapping of images instead of amplitude spectra as in Ito's method(2006). Firstly, the amplitude spectra of the registered image and input image are calculated:  $|F(k_1, k_2)|$   $|G(k_1, k_2)|$ . In the low-frequency domain, however, because most energy is concentrated in case of natural images, it is better to calculate  $\log|F(k_1, k_2)|$  and  $\log|G(k_1, k_2)|$  (Takita, 2003). Secondly, the log-polar mapping  $-|F_{LP}(k_1, k_2)|$   $|G_{LP}(k_1, k_2)|$  is calculated to estimate the rotation angle  $\theta$  between  $|F_{LP}(k_1, k_2)|$   $|G_{LP}(k_1, k_2)|$ . The last step is similar to the Ito's method(2006). Although Takita(2003) proposed an algorithm to estimate the rotation angle and translational displacement by using fitting the analytical model and a spectrum weighting mentioned in the recognition of partial shoeprints(Gueham, Bouridane and Crookes, 2007), the project just applies the idea of log -polar mapping to the straightforward method of Ito(2006) in order to improve the high accuracy of the project.

Moreover, in order to reduce the effect of background components in image, Ito(2006) applied 2D spatial window to these image before estimating stages. The project combines these ideas for proposing algorithm of recognition palmprint, which consists of determine the size of frequency spectrum, estimation rotation and translation, calculating log-polar mapping and applying the Hanning Window(Ito, 2004; Takita, 2003; Ito, 2006). The details of the method are presented in the next sections.

## 2.4 Property of shift invariance

This section will explain more clearly the property of shift invariance, which is used to estimate the translational displacement between images by using DFTs instead of direct calculation.

Let  $g_1(n_1, n_2)$  be the displaced version of the original image  $g(n_1, n_2)$ . The  $g_1(n_1, n_2)$  is given by:

$$g_1(n_1, n_2) = g(n_1 + \tau_1, n_2 + \tau_2),$$

By applying the DFTs to the above equation the following can be obtained:

$$G_1(u, v) = e^{-j2\pi(\tau_1 u + \tau_2 v)} G(u, v)$$

The POC function  $r_{fg_1}(n_1, n_2)$  between  $g_1(n_1, n_2)$  and  $f(n_1, n_2)$  will be given by:

$$\begin{aligned} r_{fg_1}(n_1, n_2) &= \frac{1}{N_1 N_2} \sum_{k_1, k_2} e^{j(\theta(k_1, k_2) - \frac{2\pi\tau_1 n_1}{N_1} - \frac{2\pi\tau_2 n_2}{N_2})} x W_{N_1}^{-k_1 n_1} W_{N_2}^{-k_2 n_2} \\ &\cong r_{fg}(n_1 + \tau_1, n_2 + \tau_2) \end{aligned}$$

The above equation shows that the correlation peak is shifted by  $(\tau_1, \tau_2)$  and the value of the peak is invariant with respect to the positional image translation and illumination changes. Therefore, the image shift  $(\tau_1, \tau_2)$  can be estimated by detecting the location of the correlation peak.

In this part, the way how to determine the translational displacement by using POC function is presented in detail. However, the complete discussion of the DFTs of the image in POC functions will be presented in chapter 4 in which techniques applied to the image.

## 3 Chapter 3. Review of some existing palmprint recognition algorithms

In this chapter, in order to compare with the method based on Phase-Only Correlation, two existing palmprint recognition algorithm using other different techniques are investigated, which are Zhang's algorithm (2003) and Kumar's algorithm (2004) using real and complex Gabor filter masks, respectively. A deep discussion of the method how to extract the Region of Interest(ROI) of the palmprint is also presented in the last section.

### 3.1 2D Gabor phase encoding scheme

#### 3.1.1 Feature extraction and coding

In addition to a new tool for online palmprint image acquisition, Zhang (2003) proposed a 2D Gabor phase encoding scheme as a new tool for acquiring palmprint image online. The main purpose of the method is to extract and represent texture features of a low-resolution palmprint. Having been used for iris recognition (Daugman, 1993), the circular Gabor filter is an efficient approach for analyzing texture, given by

$$G(x, y, \theta, u, \sigma) = \frac{1}{2\pi\sigma^2} \exp\left\{-\frac{x^2 + y^2}{2\sigma^2}\right\} \exp\{2\pi i(ux\cos\theta + uy\sin\theta)\},$$

Where  $I = \sqrt{-1}$ ,  $u$  is the sinusoidal - wave frequency,  $\theta$  controls the function orientation, and  $\sigma$  is the standard deviation of the Gaussian envelope.

$G(x, y, \theta, u, \sigma)$ , is turned to zero DC (direct current) with the application of the following formula, which is helpful to make it more robust against brightness:

$$\tilde{G}[x, y, \theta, u, \sigma] = G[x, y, \theta, u, \sigma] - \frac{\sum_{i=-n}^n \sum_{j=-n}^n G[i, j, \theta, u, \sigma]}{(2n+1)^2},$$

Where  $(2n + 1)^2$  is the filter size. Normally, due to add symmetry, the imaginary part automatically returns zero, and the adjusted Gabor filter is used to filter the image during preprocessing(Zhang, 2003).

A turning process is applied to optimize the selection of three parameters,  $\theta$ ,  $\sigma$ , and  $u$ , which have a direct effect on the achievement of 2D Gabor phase coding (Zhang,



2003). Consequently, a feature vector with 2,048 dimensions is generated by one Gabor filter exploited with optimized parameters,  $\theta = \frac{\pi}{4}$ ,  $u = 0.0916$ , and  $\sigma = 5.6179$ . Moreover, in order to handle the palmprint misplacement, an automatic thresholding procedure is used during data sampling. Occasionally, several non-palmprint pixels are included in the images because of the incorrect place of the hand, and thus a mask generated for determining the nonpalmprint pixels location, which is useful to remove such redundant information from the image (Zhang, 2003). Then, a threshold can be used easily to segment these nonpalmprint pixels, which also is applied for transferring to a binary image in extraction processing (Zhang, 2003). Instead of using an automatic thresholding, the project gives each image a fixed thresholding which can reduce the time of processing but can give negative impacts on the results. Actually, choosing a suitable thresholding is not investigated and gets less paid attention in the project despite of important roles.

### 3.1.2 Palmprint matching

In order to determine the similarity degree between training database and testing database, a normalized Hanning distance is adopted with feature vectors representing data consisting of two matrices, real and imaginary (Daugman, 1993; Zhang, 2003). Let  $P$  and  $Q$  be two palmprint feature vectors. The normalized hamming distance can be described as

$$D_o = \frac{\sum_{i=1}^N \sum_{j=1}^N P_M(i,j) \cap Q_M(i,j) \cap (P_R(i,j) \otimes Q_R(i,j)) + P_M(i,j) \cap Q_M(i,j) \cap (P_I(i,j) \otimes Q_I(i,j))}{2 \sum_{i=1}^N \sum_{j=1}^N P_M(i,j) \cap Q_M(i,j)},$$

Where  $P_R(Q_R)$ ,  $P_I(Q_I)$ , and  $P_M(Q_M)$  are the real part, the imaginary part and the mask of  $P(Q)$ , respectively.

For the best matching, the hamming distance should be zero. Zhang (2003) needed to vertically and horizontally translate one of the features and matching again due to defective preprocessing. The ranges of the vertical and horizontal translations are defines form -2 to 2. The final matching score is the minimum  $D_o$  value obtained from the translated matching. Contrast to the algorithm based on Phase-Only Correlation, the preprocessing including rotation, scaling and translation is extremely important because the high-accuracy of matching depends on straightforwardly the preprocessed image (Ito, 2006; Takita, 2003; Ito, 2008).

### 3.2 Palmprint identification using PalmCodes

Kumar and Shen(2004) argued the results of Zhang's algorithm(2003) biased and thus not represent the actual performance. Contrast to Zhang's (2003), firstly, during the image acquisition the palmprint rotation and translation was restricted as the marks of alignments. Secondly, Kumar and Shen(2004) showed that the combining of two palmprint make the performance better than the utilizing separate these palmprints. They also stated that it was impossible to estimate the equivalent performance for two subjects by using the combination of two same-subject palmprints. Finally, Zhang (2003) used complex Gabor functions in the palmprint identification system with the single palmprint, Kumar and Shen(2004) used real Gabor function to capture its salient features because it is necessary to extract automatically the region of interest in any palmprint-based identification system would require automated extraction of region of interest(Kumar and Shen, 2004).

The figure 3.1 shows completely the recognition system stages. After selected from the users, the palmprint are normalized to reduce the brightness because of sensor noise as well as variations in palm pressure. By a bank of RGF filters, the normalized images is filtered in order to compute the salient features in several concentric overlapping bands. The similarity measure between corresponding feature vectors is used for achievement of the palmprint identification. Here are some formulas used in the method(Kumar and Shen, 2004):

#### 3.2.1 Normalization

The extracted palmprint images normalized has simpler computation and thus make it sufficient to acquire inkless images. The mean ( $\emptyset$ ) and the variance ( $\rho$ ) of image  $I(i, j)$  are used to compute the normalized image ' $i, j$ ) :

$$I'(i, j) = \begin{cases} \emptyset_d + \lambda & \text{if } I(i, j) > 0 \\ \emptyset_d - \lambda & \text{otherwise} \end{cases}$$

$$\text{Where } \lambda = \sqrt{\frac{\rho_d \{xI(i, j) - \emptyset\}^2}{\rho}}$$

Where  $\emptyset_d$  and  $\rho_d$  are the desired values for mean and variance.

### 3.2.2 Multichannel filtering

By an oriented cosine function, in the spatial domain, the RGF filter is a Gaussian function modulated. The impulse response RGF in 2D plane has following general form:

$$h(x', y') = \exp \left[ -\frac{1}{2} \left( \frac{x'^2}{\sigma_x^2} + \frac{y'^2}{\sigma_y^2} \right) \right] \cos(2\pi u_0 x')$$

where  $x' = x \sin\varphi + y \cos\varphi$ ;  $y' = x \cos\varphi - y \sin\varphi$  and  $u_0$  denotes the radial frequency of sinusoidal plane wave along direction  $\varphi$  from  $x$  axis. The space constants  $\sigma_x$  and  $\sigma_y$  define the Gaussian envelope along  $x$  and  $y$ -axes respectively.

These were set as;  $u_0 = 1/10$ , and  $\sigma_x = \sigma_y = 4$ . The RGF filters were implemented as  $13 \times 13$  spatial masks with six different values. This can help the computational complexity of Kumar's method to be a half of that in Zhang's (Kumar and Shen, 2004).

### 3.2.3 Extraction of features

The usage of circular concentric bands was motivated by ring projection algorithm (Tsai and Chiang, 2002) which can be useful to achieve rotational invariance. Because it is possible to reduce the effects of palm stretching by using the overlapping of concentric circular bands, Kumar and Shen (2004) used the variance and mean of gray levels in the concentric circular bands to capture the significant features. The mean value of ring projection vectors for every filtered image,  $I'_\varphi(i, j)$  in the circular band between radius  $r_1$  and  $r_2$  is given by:

$$\mu_\varphi^p = \frac{1}{N_r} \sum_r \sum_q I'_\varphi(r \cos\theta_q, r \sin\theta_q), p = 1, 2, \dots, Z$$

Where  $Z$  is the circular-band total number and  $N_r$  is pixel number falling between the circle of radius  $r_1$  and  $r_2$ . The variance of local gray level pixels is given by:

$$\sigma_\varphi^p = \sqrt{\frac{1}{N_r^2} \sum_r \sum_q (I'_\varphi(r \cos\theta_q, r \sin\theta_q) - \mu_\varphi^p)^2}$$

A unique feature vector is obtain by using the set of the above features orders from each of the filtered images, which is referred to as PalmCode similar to *FingerCode* or *IrisCode* used in the literature(Daugman, 1993).

is given by:

$$\Omega_k = \{\mu_\varphi^p, \sigma_\varphi^p\} \quad \forall p = 1, 2, \dots, Z, \varphi = 0^\circ, 30^\circ, \dots, 150^\circ$$

### 3.2.4 Identification

The *PalmCodes* for every possible user, from their palmprint training images, is used to build training database or matrix  $\Omega$ , *i.e.*

$$\Omega = [\Omega_1, \Omega_2, \dots, \Omega_N]$$

where  $N$  is the valid-user number. The maximum similarity between the feature vectors in matrix  $\Omega$  and query vector  $\Omega$  is calculated by:

$$\beta_{max} = \max_k \left\{ \frac{\sum_l \Lambda \Omega_k}{\sqrt{\sum_l \Lambda \sum_l \Omega_k}} \right\}, l = 1, 2, \dots, 6Z, k = 1, 2, \dots, N.$$

The generate highest score  $\beta_{max}$ , is assigned to the *PalmCode*  $\Lambda$  of unknown user.

In conclusion, the computational complexity of the proposed method is about half that of method in Zhang's paper (2003) mainly due to the usage of RGF mask of size 13 x 13 instead of complex Gabor filter masks of 31x 31 sizes used in Zhang' algorithm. The reliability on the performance of a personal recognition system largely depends on its degree of tolerance due to rotation, translation, and scaling. Although, the palmCode representation used Kumar and Shen(2004) is not rotation invariant, the rotation is well handled by the rotation of PalmCode during the verification/recognition stages. In other words, the preprocessing of Kumar (2004) is better than Zhang's (2003) in terms of rotation and translation. However, in order to extract the ROI, the method of Zhang's is used more regularly than Kumar's (Ito, 2004; Ito, 2006; Gueham, 2007), which is presented in the next section.

## 3.3 Extraction of region of interest

This section is concerned with with a brief description of existing methods for extracting region of interest using Kuma's method and Zhang's method and identifies the most sufficient technique for modifying the ROI extraction method as the combination of Zhang's and Kuma's.

### 3.3.1 Kuma's

The role of this part is to determine the effective area of the pamlprint assumed as the composite hand images with the uniform background (Kumar, 2004). In order to binarized, the image is subjected to the discriminate analysis by using the image histogram. A histogram of the image is created when the pixel number which have a specific grey level value (Petrou and Bosdogianmi, 1999). Properly normalized, the

histogram is essentially the probability density function for a certain grey level value to occur.

In addition, during the acquisition of images, being used subsequently, the thresholding limit computed only for one image due to the relative constant of the background and lighting conditions. In order to compute the region of interest, the binarized image is subjected to the morphological erosion (Kumar, 2004). Indeed, let  $R$  be the set of non-zero pixels in a given binary image and  $SE$  be the set of non-zero pixels *i.e.* structuring element. The morphological erosion is defined as:

$$R \ominus SE = \{g: SE_g \subseteq R\}$$

where  $g$   $SE$  denotes the structuring element with its reference point shifted by  $g$  pixels. A square structuring element ( $SE$ ) is used to probe the composite binarized image. The center of this residual image enclosing the residue is determined, which are used to extract a circular palmprint region of fixed size from the composite hand image.

### 3.3.2 Zhang's

Step 1. Gaussian smoothing- a low pass filter is applied to the original image to reduce the noise. Then, by using a threshold, the convolved image is converted to a binary image, which is useful to determine the boundary of the image.

Step 2. Using a boundary tracking algorithm of Gonzalez (2008), the boundary of the binary image is obtained for finding the areas between the fingers. Contrast to Zhang's method (2003), the boundary of the gap between the ring and middle fingers is extracted since it is useful for the following processing.

Step 3. The tangent of the two gaps is computed. Let  $(x_1, y_1)$  and  $(x_2, y_2)$  be any points on  $(F_{x_j}, F_{y_j})$  respectively. If the line  $(y = mx + c)$  passing through these two points satisfies the inequality,  $F_{y_j} \leq mF_{x_j} + c$  for all  $j$ , then the line  $(y = mx + c)$  is considered to be the tangent of the two gaps.

Step 4: Line up  $(x_1, y_1)$  and  $(x_2, y_2)$  to get the Y-axis of the palmprint coordinate system, .The line passing through the midpoint of these two points is determined, that is helpful to the center of the region of interest.

Step 5: Located at a certain area of the palmprint image, a subimage of a fixed sized (128x128) is extracted based on the coordinate system. Therefore, the region of interest has been extracted.

Figure 3.2 shows the completely procedure and the difference between the Zhang's method and the project's.

## 4 Chapter 4: Principles of DFTs and image processing techniques in palmprint recognition.

This chapter presents brief theory basics of image processing techniques in Discrete Fourier Transform, including the periodicity and display of DFTs, and the DFTs of the rotated image, shifted image used for calculating the POC function. What's more, in order to create effectively a ROI- database used for the matching stage in proposed method, three techniques, including a low pass filter, a threshold and a boundary tracking are discussed in the section.

### 4.1 Hanning Window:

Due to the DFT periodicity explained in the next section, an image can be considered to “wrap around” at an edge, and therefore discontinuities, which are not supposed to exist in real word, occur at every edge in 2D DFT computation(Ito, 2006; Takita, 2003). The effect of discontinuity at image border is reduced by applying 2D window function to the input images  $f(n_1, n_2)$  and  $g(n_1, n_2)$ . For this purpose, 2D Hanning window is defined by

$$w(n_1, n_2) = \frac{1 + \cos(\frac{\pi n_1}{M_1})}{2} \frac{1 + \cos(\frac{\pi n_2}{M_2})}{2}$$

The figure 4.1 shows the images applied Hanning window to eliminate the effect of periodicity in DFT which is discussed in section 4.2.1.

### 4.2 The 2-D Discrete Fourier Transform and its Inverse.

The 1-D discrete Fourier transform of a function  $f(x)$  defined at discrete points  $x$ , is defined as (Gonzalez, 1992; Gonzalez, 2008):

$$F(u) = \sum_{x=0}^{M-1} f(x) e^{-j2\pi(\frac{ux}{M})} \quad u = 0, 1, 2, \dots, M-1 \quad (1.0)$$

The Discrete Fourier Transform (DFT) of one variable would yield the following 2D-Discrete Fourier transform (DFT)(Gonzalez, 1992; Gonzalez, 2008):

$$F(u, v) = \sum_{x=0}^{M-1} \sum_{y=0}^{N-1} f(x, y) e^{-j2\pi(\frac{ux}{M} + \frac{vy}{N})} \quad (1.1)$$

Where  $f(x, y)$  is a digital of size  $M \times N$ . As in the 1D case (Gonzalez, 2008), the above equation must be evaluated for values of discrete variables  $u$  and  $v$  in the ranges  $u = 0, 1, 2, \dots, M-1$  and  $v = 0, 1, 2, \dots, N-1$ . Given the transform  $F(u, v)$ , we can obtain  $f(x, y)$  by using the inverse discrete Fourier transform (IDFT):

$$f(x, y) = \frac{1}{MN} \sum_{u=0}^{M-1} \sum_{v=0}^{N-1} F(u, v) e^{j2\pi(\frac{ux}{M} + \frac{vy}{N})} \quad (1.2)$$

For  $x = 0, 1, 2, \dots, M-1$  and  $y = 0, 1, 2, \dots, N-1$ . Equations (1.1) and (1.2) constitute

The 2-D discrete Fourier transforms pair (Gonzalez, 1992; Gonzalez, 2008). The rest of Phase- Only Correlation in this project is based on properties of these two equations and their use for image flirting in the frequency.

Sometimes, it is found that the  $1/MN$  constant in front of DFT instead of the IDFT (Gonzalez, 1992; Gonzalez, 2008). At times, the constant is expressed as  $1/\sqrt{M \cdot N}$  and it's included in front of the forward and inverse transforms, thus creating a more symmetric pair (Petrou and Bosdogianni, 1999). Gonzalez (2008) stated that any of these formulations was correct

Several properties of the 2-D discrete Fourier transform and its inverse.

#### 4.2.1 Periodicity

The 2-D Fourier transform and its inverse are infinitely periodic in the  $u$  and  $v$  directions; that is,

$$F(u, v) = F(u + k_1 M, v) = F(u, v + k_2 N) = F(u + k_1 M, v + k_2 N)$$

And

$$f(x, y) = f(x + k_1 M, y) = f(x, y + k_2 N) = f(x + k_1 M, y + k_2 N)$$

Where  $k_1$  and  $k_2$  are integers.

The transform data in the interval from 0 to  $M-1$  consists of two back-to-back half periods meeting at point  $M/2$  (Gonzalez, 2008). For display and filtering purposes, it is more convenient to have in this interval a complete period of the transform, in



which the data are contiguous. The periodicities of transform and its inverse are important issues in the implementation of DFT-based algorithms. Consider the 1-D spectrum as a simple explanation with the equation given by:

$$f(x)e^{j2\pi(\frac{u_0x}{M})} \Leftrightarrow F(u - u_0)$$

In other words, multiplying  $f(x)$  by the exponential term shown shifts the data so that the origin  $F(0)$ , is located at  $u_0$ . If  $u_0 = \frac{M}{2}$ , the exponential term becomes  $e^{j\pi x}$  which is equal to  $e^{j2\pi}$  which is equal to  $(-1)^x$  because  $x$  is an integer. In this case,

$$f(x) (-1)^x \Leftrightarrow F(u - \frac{M}{2})$$

That is, multiplying  $f(x)$  by  $(-1)^x$  shifts the data so that  $F(0)$  is at the centre of the interval  $[0, M - 1]$ .

In 2-D, instead of two half periods, there are now four quarter periods meeting at the point  $(\frac{M}{2}, \frac{N}{2})$  ([Gonzalez, 2008]). The dashed rectangles correspond to the infinite number of periods of the 2-D DFT. As in the 1-D case, visualization is simplified if we shift the data so that  $F(0, 0)$  is at  $(\frac{M}{2}, \frac{N}{2})$ . Letting  $(u_0, v_0) = (\frac{M}{2}, \frac{N}{2})$  in Eq. (1.3) results in the expression

$$f(x, y) (-1)^{x+y} \Leftrightarrow F(u - \frac{M}{2}, v - \frac{N}{2})$$

Using this equation shifts the data so that  $F(0, 0)$  is at the center of the frequency rectangle by the intervals  $[0, M - 1]$  and  $[0, N - 1]$ , as desired.

Figure 4.2 shows the results of the periodicities of the 2-D Fourier transform and its inverse.

#### 4.2.2 The DFTs of the rotated image.

Indeed, for simplicity, set  $M = N$ , the definition of the discrete Fourier transform Eq.

(1.1) for a square image:

$$F(u, v) = \sum_{x=0}^{N-1} \sum_{y=0}^{N-1} f(x, y) e^{-j2\pi(\frac{ux+vy}{N})} \quad (1.5)$$

The polar coordinated are in

roduced on the plane  $(x, y)$  and  $(u, v)$  as follows (Gonzalez, 2008; Petrou and Bosdogianni, 1999):

$$x = r \cos \theta \quad y = r \sin \theta \quad u = w \cos \varphi \quad v = w \sin \varphi$$

Petrou and Bosdogianni (1999) noted that:

$ux + vy = rw(\cos \theta \cos \varphi + \sin \theta \sin \varphi) = rwc \cos(\theta - \varphi)$ . Then Eq. (1.5) becomes:

$$F(w, \varphi) = \sum_{x=0}^{N-1} \sum_{y=0}^{N-1} f(r, \theta) e^{-j2\pi \left( \frac{rwc \cos(\theta - \varphi)}{N} \right)} \quad (1.6)$$

Suppose now that  $f(r, \theta)$  is rotated by an angle  $\theta_0$ . It becomes  $f(r, \theta + \theta_0)$ . The requirement if to find the discrete Fourier transform of this rotated function. The formula (1.6) is used to calculate the DFT of  $f(r, \theta + \theta_0)$  by simply replacing  $f(r, \theta)$  by  $f(r, \theta + \theta_0)$ . The DFT of  $f(r, \theta + \theta_0)$  by  $F'(w, \varphi)$

$$F'(w, \varphi) = \underbrace{\sum \sum f(r, \theta + \theta_0)}_{\text{all points}} e^{-j2\pi \left( \frac{rwc \cos(\theta - \varphi)}{N} \right)} \quad (1.7)$$

In order to find the relationship between  $F'(w, \varphi)$  and  $F(w, \varphi)$ , a new variable  $\theta' \equiv \theta + \theta_0$ . The Eq. (1.7) is rewritten as follows:

$$F'(w, \varphi) = \underbrace{\sum \sum f(r, \theta')}_{\text{all points}} e^{-j2\pi \left( \frac{rwc \cos(\theta' - \theta_0 - \varphi)}{N} \right)}$$

Therefore, on the right hand side of the above formula, the DFT of the unrotated image calculated at  $\varphi + \theta_0$  instead of  $\varphi$ . That is,

$$F'(w, \varphi) = F(w, \varphi + \theta_0)$$

The DFT of the image rotated by  $\theta_0$  equals to then DFT of the unrotated image rotated by the same angle  $\theta_0$  (Petrou and Bosdogianni, 1999). In other words, rotating  $f(x, y)$  by an angle  $\theta_0$  rotates  $F(u, v)$  by the same angle. Conversely, rotating  $F(u, v)$  rotates  $f(x, y)$  by the same angle (Gonzalez, 2008):

$$f(r, \theta + \theta_0) \Leftrightarrow F(w, \varphi + \theta_0)$$

#### 4.2.3 The DFTs of the shifted image

Suppose that the image is shift to the point  $(x_0, y_0)$ , so that it becomes  $f(x - x_0, y - y_0)$ . To calculate the DFT of the shift image, the DFT of  $f(x - x_0, y - y_0)$  is denoted by  $F'(u, v)$  given by:

$$F'(u, v) = \sum_{x=0}^{N-1} \sum_{y=0}^{N-1} f(x - x_0, y - y_0) e^{-j2\pi(\frac{ux+vy}{N})}$$

To find a relationship between  $F'(u, v)$  and  $F(u, v)$ ,  $f(x, y)$  is made appear on the right hand side of this expresiong. For this purpose, Two new variable are defined:

$$x' \equiv x - x_0, \quad y' \equiv y - y_0$$

$F'(u, v)$  is rewritten by:

$$F'(u, v) = \sum_{x'=-x_0}^{N-1-x_0} \sum_{y'=-y_0}^{N-1-y_0} f(x', y') e^{-j2\pi(\frac{ux'+vy'}{N})} e^{-j2\pi(\frac{ux_0+vy_0}{N})}$$

Because of the assumed periodic repetition of the image in all direction, where exactly we perform the summation(i.e. between which indices) does not really matter, as long as the right sized window is used for the summation(Petrou and Bosdogianni, 1999). In other words, as long as summation indices  $x'$  and  $y'$  are

allowed to take  $N$  consecutive values each, it does not matter where they start from.

Therefore, in the expression above,  $x'$  and  $y'$  are assumed to take value from 0

to  $N - 1$ . It is noticed that the factor  $e^{-j2\pi(\frac{ux_0+vy_0}{N})}$  is independent of  $x'$  and  $y'$  and thus can come out of the summation (Petrone and Bosdogianni, 1999). The relationship between  $F'(u, v)$  and  $F(u, v)$  is given by:

$$F'(u, v) = F(u, v) e^{-j2\pi(\frac{ux_0+vy_0}{N})}$$

Therefore, it can be shown by direct substitution into Eqs.(1.1) and (1.2) that the Fourier transform pair satisfies the following translation properties(Gonzalez, 2008):

$$f(x, y)e^{j2\pi(\frac{u_0x}{M}+\frac{v_0y}{N})} \Leftrightarrow F(u - u_0, v - v_0) \quad (1.3)$$

And  $u_0$

$$f(x - x_0, y - y_0) \Leftrightarrow F(u, v)e^{-j2\pi(\frac{x_0u}{M}+\frac{y_0v}{N})} \quad (1.4)$$

That is, multiplying  $f(x, y)$  by the exponential shown shifts the origin of the DFT to  $(u_0, v_0)$  and, conversely, multiplying  $F(u, v)$  by the negative of that exponential shifts the origin of  $f(u, v)$  to  $(x_0, y_0)$  (Petrone and Bosdogianni, 1999; Gonzalez, 2008). Translation has no effect on the magnitude (spectrum) of  $F(u, v)$ .

#### 4.2.4 The display of the image's DFTs

Because these following sections are illustrated by images and their Fourier spectra displayed as intensity function, some comments concerning these display are in order before beginning discussion of Fourier transform properties. The dynamic range of Fourier spectra usually is much higher than the typical display device is able to reproduce faithfully, in which case only the brightest parts of the image are visible on the display screen (Gonzalez and Woods, 1992). Indeed, suppose that the discrete

Fourier transform of an image is  $F(u, v)$ . These quantities,  $F(u, v)$ , are the coefficients of the expansion of the image into discrete Fourier functions each of which corresponds to a different pair of spatial frequencies in the 2- dimensional  $(x, y)$  plane. As  $u$  and  $v$  increase, the contribution of these high frequencies to the images becomes less and less important and thus the values of the corresponding coefficients  $F(u, v)$  become smaller (Petrou and Bosdogianni, 1999). It may be difficult to display these coefficients because their values will span a great range. Therefore, for displaying purposes, and only for that people use instead the logarithmic function (Gonzalez and Woods, 1992; Petrou and Bosdogianni, 1999)

$$F_L(u, v) \equiv \log(1 + |F(u, v)|)$$

This function is then scaled into a displayable range of grey values and displayed instead of  $F(u, v)$ . Notice that when  $F(u, v) = 0$ ,  $F_L(u, v) = 0$  too. This function has the property of reducing the ratio between the high value of  $F(u, v)$  and the small ones, so that small and large values can be displayed in the same scale. For example, if  $F_{\max} = 10$  and  $F_{\min} = 0.1$ , to draw these numbers on the same graph is rather difficult, as their ratio is 100. However,  $\log(11) = 1.041$  and  $\log(1.1) = 0.041$  and their ratio is 25. So both numbers can be drawn on the same scale more easily.

#### Fourier Spectrum and Phase Angle (Gonzalez, 2008)

Because the 2-D DFT is complex in general, it can be expressed in polar form:

$$F(u, v) = |F(u, v)|e^{j\phi(u, v)}$$

Where the magnitude

$$|F(u, v)| = [R^2(u, v) + I^2(u, v)]^{1/2}$$

Is called the Fourier (or frequency) spectrum, and

$$\phi(u, v) = \arctan \left[ \frac{I(u, v)}{R(u, v)} \right]$$

Is the phase angle.  $\text{atan2}(\text{Imag}, \text{Real})$

Finally, the power spectrum

$$P(u, v) = |F(u, v)|^2 = R^2(u, v) + I^2(u, v)$$

As before,  $R$  and  $I$  are the real and imaginary part of  $F(u, v)$  and all computations are carried out for the discrete variables  $u = 0, 1, 2, \dots, M - 1$  and  $v = 0, 1, 2, \dots, N - 1$ .

Therefore,  $|F(u, v)|$ ,  $\phi(u, v)$ , and  $P(u, v)$  are arrays of size  $M \times N$ .

Figure 4.3 illustrates the display DFT of the image.

#### 4.2.5 A Lowpass filter- Gaussian smoothing

The most common type of noise in images is Gaussian (Petrou and Bosdogianni, 1999). We can remove Gaussian noise by smoothing the image (Gonzalez and Woods, 2008). A lowpass filtering is much more effective for the Gaussian noise (Petrou and Bosdogianni, 1999; Gonzalez and Woods, 2008; Zhang, 2003).

*Why does lowpass filtering reduce noise?*

Usually, the noise which is superimposed on the image is uncorrelated. This means that it has a flat spectrum. On the other hand, most images have spectra which have higher value in the low frequencies and gradually reducing values for high frequencies. After a certain frequency, the spectrum of a noise signal is dominated by the noise component. Therefore, if a lowpass filter is used, all the noise-dominated high-frequency components are killed off. At the same time, of course, the useful information of the image is also killed in these high frequencies. The result is a clean, but blurred image.

#### 4.2.6 Threshold binary image

This chapter is about those Image Processing techniques that are used in order to prepare an image as an input to an automatic vision system. These techniques perform image segmentation and edge detection (Petrou and Bosdogianmi, 1999), and their purpose is to extract information from an image in such a way that the output image contains much less information than the original one, but the little information it contains is much more relevant to the other moguls of an automatic vision system than the discarded information.

One of the simplest methods is that of histogramming and thresholding (Petrou and Bosdogianmi, 1999). A histogram of the image is created when the number of pixels which have a specific grey level value. Properly normalized, the histogram is essentially the probability density function for a certain grey level value to occur.

To extract an object in an Image is to identify the pixels that make it up (Petrou and Bosdogianmi, 1999). To express information, an array of the same size as the original image is created.

In one or more dimensions, the selection of threshold values discussed so far has been manual. An operator interactively sets the cutoff values so that the resulting image is visually satisfying and the correspondence between what the user sees in the image and the pixels the thresholds select is as close as possible. This is not always consistent from one operator to another, or even for the same person over a period of time. The difficulty and variability of thresholding represents a serious source of error for further image analysis(Russ, 1999)

There are two slight different requirements for setting threshold values. Both have to do with the typical use of binary images for feature measurement. One is to achieve reproducibility, so that variation due to the operator, light, etc. do not affect the results (Russ, 1999). The second goal of setting threshold values is to achieve accurate boundary delineation. In this project, a threshold is used to convert a convolved image to boundary image. For quality-control work, this latter requirement of accuracy is somewhat less important than precision.

Since pixel-based images represent at best an approximation to the continuous real scene being represented, and since thresholding classifies each pixel as either part of

the foreground or the background, only a certain level accuracy can be achieved. An alternate representation of features based on the boundary line can be more accurate (Russ, 1999). This is a polygon with many sides and corner points defined as x, y coordinates of arbitrary accuracy, as compared to the comparatively coarse pixel spacing (Russ, 1999).

The boundary-line representation is superior for accurate measurement because the line itself has no width (Russ, 1999). However, determining the line is far from easy. The location of individual points can be determined by interpolation between pixels, perhaps fitting mathematics functions to pixel on either side of the boundary to improve the results (Russ, 1999).



## 5 Chapter 5: A proposed algorithm of palmprint recognition

In this chapter, a palmprint recognition algorithm using Phase-Only correlation is proposed by combining basic ideas from Ito (2003) with the ROI extracting technique of Zhang (2003) and the estimation rotation angle of Takita(2003).

The input of the procedure is a stored palmprint image  $f(n_1, n_2)$  and a pamlprint image  $g(n_1, n_2)$  which to be verified.

The output of the procedure is the degree of the similarity.

The basic theory of the algorithm is presented in the previous chapters.

The proposed algorithm consists of the three stages including preprocessing, extraction of ROI and palmprint matching. The Preprocessing stage is used to normalize the images rotation and/or translation(as presented in the section 5.1) are computed and used for alignment purposed. The extraction of Region of interest (ROI) is modified from the method in Zhang's paper, introduced in section 5.2. The palmprint matching stages is used the method in Ito's paper (2006).

### 5.1 The preprocessing stage

In this section, the stored image  $f(n_1, n_2)$  and the input image  $g(n_1, n_2)$  are normalized for performance of the high accuracy palmprint matching. A set of rotated images  $f(n_1, n_2)$  of the registered palmprint  $f(n_1, n_2)$  is generated over the range from -3% to 3% with each time of rotation increased 1 degree.

In order to reduce the effect of background components in palmprint images, the 2D Hanning window is applied at the center of gravity of each palmprint(figure 5.1), (figure 4.1 shows the result of a image applied 2D Hanning window).

The DFTs of each rotated register image  $f(n_1, n_2)$  and the input image  $g(n_1, n_2)$  is calculate to obtain  $F(k_1, k_2)$  and  $G(k_1, k_2)$ .

Then, the amplitude spectrum is determine as the log of the abs of the  $F(k_1, k_2)$  and  $G(k_1, k_2)$ (figure 5.2).

Next, the log-polar mapping  $|F(k_1, k_2)|$  and  $|G(k_1, k_2)|$  is calculated in order to calculate the matching  $R$  (figure 5.3).

The highest value peak of  $R$  is considered as the matching result between the rotated registered image and the input image.

The rotation angle of the rotated registered image having the highest matching with the input image is used to normalize the registered image.

Now, a rotation angle and displacement parameters is used for the normalization of the registered image and the input image. Indeed, the registered image is rotated by the rotation angle. Next, the size of rotation-normalized registered image and the input image is extended by 1 and 2 pixels for the  $n_1$  and  $n_2$  directions, respectively. This step is useful to align the translational displacement between the two palmprint.

Finally, the registered palmprint image and the input palmprint image has been normalized.

Figure 5.4 shows the completely procedure of the preprocessing stage.

#### *5.1.1 Saving computational time:*

Practically, a set of the Hanning image and the polar image of the rotated versions of the registered palmprint image are stored in advance into a memory, which reduces the time of the processing. The Hanning rotated registered image giving the highest correlation peak is selected for the matching with the Hanning input image in the step of estimation the translation displacement. The displacements parameter is obtained as the peak location of the BLPOC function.

## **5.2 The extraction of ROI**

This stage is to extract the region of the interest of the two normalized palmprint image  $f''(n_1, n_2)$  and  $g''(n_1, n_2)$ . The original idea is from Zhang's idea, presented in the chapter 3, (section 3.3.2). This stage makes it possible for the improvement of the palmprint matching.

Firstly, the original palmprint is applied with a low pass filter such as Gaussian smoothing. Secondly, a threshold is used to convert the convolved palmprint image to a binary image (figure 3.2.b). Using a boundary tracking algorithm (Gonzalez,

2008), a boundary image is obtained for finding the gap boundary between the ring and the middle fingers, is different from Zhang's idea (figure 3.2.c), that is very useful for the next processing step.

The problem here is to determine the place of two point A and B (figure 3.2.d), which is known as the corner of the gap boundary determined in the previous step (figure 3.2.c). The perpendicular line CD to the line AB and passing through the midpoint C of two points A and B is determined to finding the centre of the region of interest. On the line Cx, the point O is determined with the condition that the distance between the point O and the midpoint of the AB is 74 pixels. Of course, the place of the point O is in the palmprint.

Using the line CD and the point O, the region of the interest is extracted as a subimage of the fixed size 128x128.

#### **5.2.1 *How can to determine the corners of the area between the ring and middle fingers.***

The idea to find the point A and B is to determine the differences between the pixels on the boundary of the image as much as possible. Particularly, with a consecutive three pixels, the coordination sum of the middle pixel is compared with the coordination sum of the others. Determining the position of A and B is understood as to find these biggest angles of the area determine the area between the ring finger and the middle finger. These points are at which the angle is less than 180%. In other words, A and B is known as any point satisfying not to be "smooth". In order to improve high accuracy in this step, it is very important to calculate the most suitable gray for transferring original image to binary image.

Figure 5.5 shows the way how to identify the points A and B as the corners of the area between the middle and ring fingers.

Figure 5.6 concludes summarily the procedure to extract the Region of interest.

### **5.3 The matching stage**

In the stage, the band-limited POC function between the two ROI is calculated for evaluation the matching score. The highest peak value is considered as the matching score.

It is noted that, for simplicity, the inherent frequency band  $K_1$  and  $K_2$  (chapter 2, section 2.1.3) in each time of calculated is considered as follows:

$$K_1/M_1 = K_2/M_2 = 0.5$$

Figure 5.7 shows the procedure of the matching stage.

## 6 Chapter 6: Evaluation of results, methods, and aims.

This chapter aims to explain how the proposed algorithm is implemented, including evaluations of results, methods, and aims.

In order to evaluate the project, the brief summary of verification and recognition scenarios with standards known as FAR, FRR, EER and ROC is presented at the beginning of the chapter.

### 6.1 Verification and recognition

#### 6.1.1 Verification: Am I who I claim to be?

*The following is taken from a paper describing definitions on verification system.*

“This scenario can be employed in a control access point application. It is used when a subject provides an alleged identity. The system then performs a one-to-one match that compares a query biometric image against the template image, of the person whose identity is being claimed, stored in the database. If a match is made, the identity of the person is verified”.

*(Boudridane, 2009)*

There are two subject groups in a verification test, clients and imposters.

Clients are defined as people trying to gain access using their own identity. The percentage of clients rejected access is reported as the False Rejection Rate (FRR).

Imposters are defined as people trying to gain access using a false identity. A false identity is an identity known to the system but not belonging to them. The percentage of imposters gaining access is reported as the False Acceptance Rate (FAR). FAR and FRR are explained in detail in the section 6.2.

#### 6.1.2 Identification/Recognition: Who am I?

*“Identification is a process of compare one image against  $N$  images” (Zhang, 2003).*

*It can be seen from this that:*

This mode is used when the identity of the individual is not known in advance. The entire template database is then searched for a match to the individual concerned in a one-to-many search. When a match is made the individual is identified. The recognition test works for the assumption that all biometric images being tested are of known persons. The percentage of correct identifications is reported as the correct (or Genuine) identification Rate (CIR) or the percentage of false identification is reported as the False identification Rate (FIR).

*(Boudridane, 2009)*

## 6.2 FAR, FRR, EER and ROC

The figures 6.1 explain more details of these definitions. For example, a biometric verification system is tested with two subject groups consisting of both impostor and client patterns.

### 6.2.1 Impostor patterns and FAR

In terms of the impostor patterns, the belonging scores are distributed around a certain mean score. Depending on the choice of the classification threshold, between all and none of the impostor patterns are falsely accepted by the system (figure 6.1.a). The threshold depending fraction of the falsely accepted patterns divided by the number of all impostor patterns is called **False Acceptance Rate (FAR)**. Its value is one, if all impostor patterns are falsely accepted and zero, if none of the impostor patterns is accepted (figure 6.1.b).

### 6.2.2 Client patterns and FRR

Similar to the impostor scores, the client pattern's scores vary around a certain mean value (figure 6.1.c). The mean score of the client patterns is higher than the mean value of the impostor patterns. If a classification threshold that is too high is applied to the classification scores, some of the client patterns are falsely rejected. Depending on the value of the threshold, between none and the entire client patterns will be falsely rejected (Figure 6.1.d). The fraction of the number of rejected client patterns divided by the total number of client patterns is called **False Rejection Rate (FRR)**. According to the FAR, its value lies in between zero and one.

The choice of the threshold value becomes a problem if the distributions of the client and the impostor scores overlap (figure 6.1.e). If the score distributions overlap, the FAR and FRR intersect at a certain point. The value of the FAR and the FRR at this point, which is of course the same for both of them, is called the Equal Error Rate (EER) (figure 6.1.f), which is calculated in the section 6.2.4.

### 6.2.3 Receiver Operating Characteristic (ROC)

Receiver Operating Characteristic (ROC) curve is used to summarize the performance of a biometric verification system. An ROC curve plots, parametrically as a function of the decision threshold, the percentage of impostor attempts accepted (i.e. false acceptance rate (FAR) =) on the x-axis, against the percentage of genuine attempts accepted (i.e. 1 - false rejection rate (FRR)) on the y-axis. The ROC curve is threshold independent, allowing performance comparison of different systems under similar conditions (Mayoue, 2007).

The Receiver Operating Characteristics (ROC) curve is depicted in the figure 6.1.f which is the plot of the FAR and FRR against all possible operation points. The curve clearly shows that the proposed technique performs well, giving an EER (FAR = FRR) of which is clearly good result.

### 6.2.4 The equal error rate (EER)

The equal error rate (EER) is computed as the point where FAR (t) = FRR (t). In practice, the score distribution is not continuous and a crossover point might not exist. Therefore, in this case, the EER value is computed as follows (Mayoue, 2007):

$$EER = \begin{cases} \frac{FAR(t_1) + FRR(t_1)}{2} & \text{if } FAR(t_1) - FRR(t_1) \leq FRR(t_2) - FAR(t_2) \\ \frac{FAR(t_2) + FRR(t_2)}{2} & \text{otherwise} \end{cases}$$

Where

$$t_1 = \max_{t \in S} \{t | FRR(t) \leq FAR(t)\}, \quad t_2 = \min_{t \in S} \{t | FRR(t) \geq FAR(t)\}$$

And S is the set of thresholds used to calculate the score distributions.

## 6.3 Evaluation of results

Experimental evaluation using the PolyU palmprint database clearly demonstrates an effective matching performance of the proposed algorithm compared directly with a featured-based algorithm, Zhang's and indirectly with Kumar's.

A set of experiments using the PolyU palmprint database are used for evaluating palmprint matching performance of the proposed algorithm. This database consists of 600 images (384 x 284 pixels) with 100 subject and 6 different palmprint images - three testing images and three training images, which are used as input images and registered images, respectively. Figure 6.2 shows an example of palmprint images in this database.

As mentioned in the section 5.1.1, the most important step of preprocessing stage is the preparation of input including the PolyU database, Hanning image, amplitude spectrum and log-polar mapping. Therefore,  $300 \times 20 = 6000$  Hanning images are calculated. These Hanning images are transferred to amplitude spectrum images and log-polar mapping, respectively. These databases are used to calculate the displacement and finding the rotation angle.

This step impacts directly to the comparison between rotated image and the registered image.

Figure 6.3 concludes the procedures of preparing database.

### 6.3.1 Verification accuracy

To obtain the verification accuracy of the proposed algorithm, each of the three testing palmprint images was matched with the other three training palmprint images in the database. A matching is noted as a correct matching if two palmprint images are from the same palm. The project first evaluates the FRR for all possible combination of client attempts: the number of attempts is  $3 \times 3 \times 100 = 900$ . Next the project evaluate the FAR for  $3 \times 100 \times 3 \times 99 = 89100$  (each testing image of a palmprint was matched with three training image of the other palmprints)

Zhang's algorithm results in at a 98% genuine accepted rate (GAR) and 4% false rate and the corresponding threshold is 0.3425 (Zhang, 2003), which compares to the proposed method: EER = 2,1071% (FAR = FRR); FAR = 2% GAR = 98% at threshold



0.4. These results also is compared to Kumar's: recognition rate = 97.50% with EER = 3.03% at a specific threshold of 0.992.

Figure 6.5 shows the results of FAR, FRR and EER.

### 6.3.2 Identification/Recognition accuracy

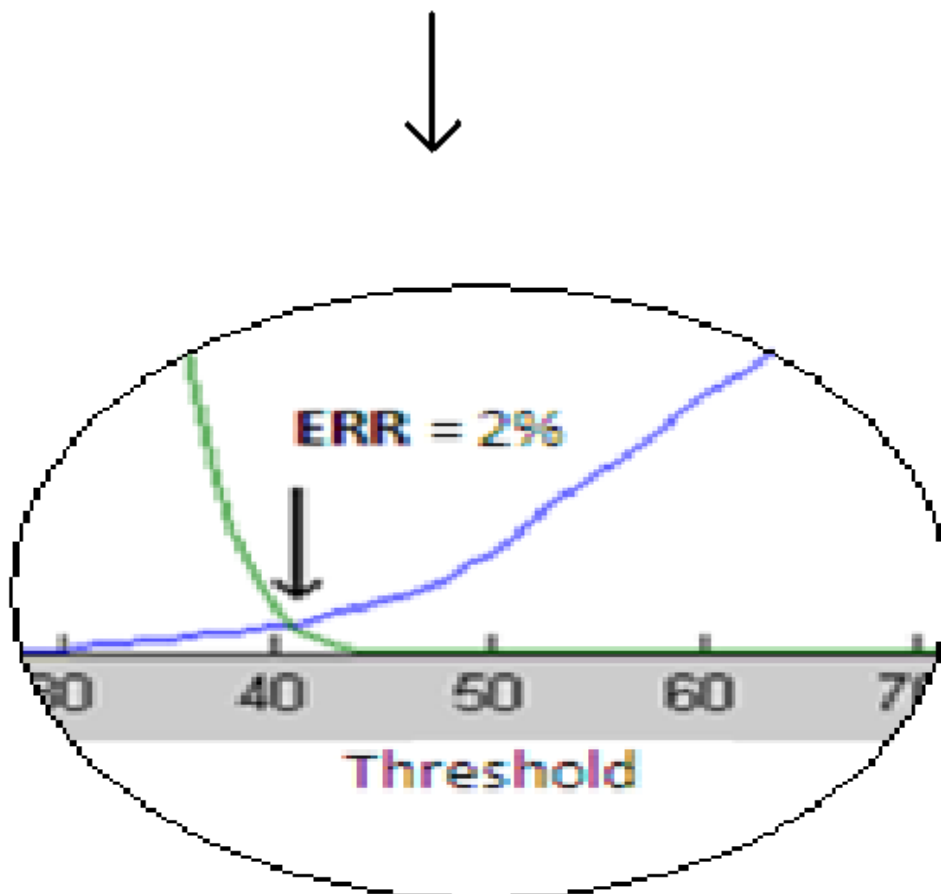
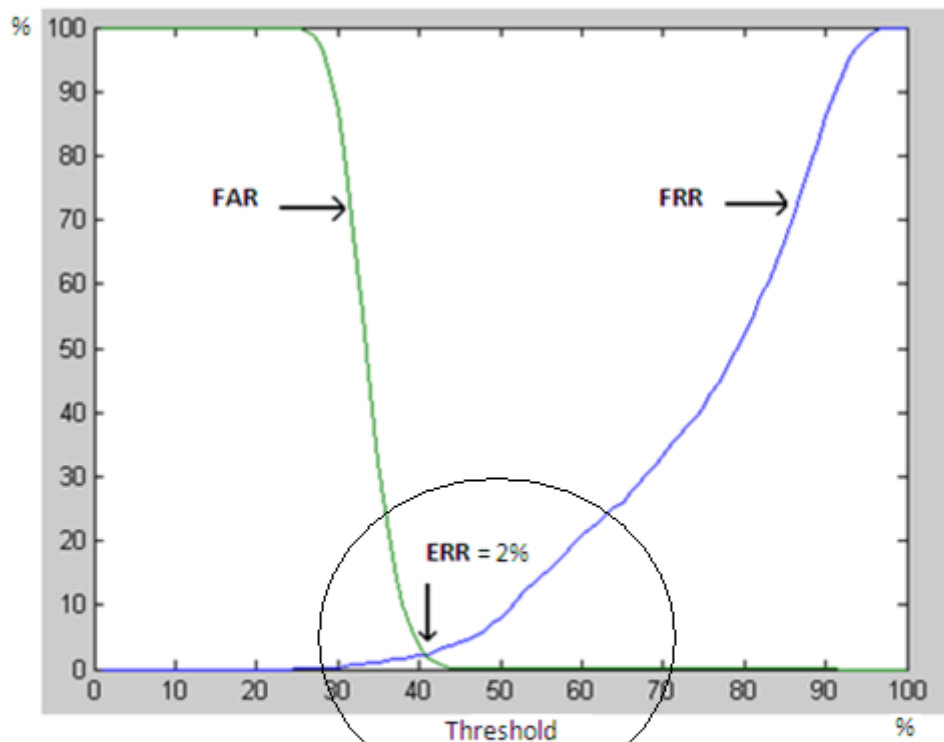
A registration database contains 300 templates from 100 different palms, where each palmprints has three templates known as training images. A testing database was setup with 300 templates from the 100 different palms introduced as testing images. None of palmprint images in the testing database are contained in any of the registration databases. Each of the palmprint images in the testing database is matched with all of the palmprint to generate incorrect and correct matching.

After mathing, the input  $g_i$  with all database images, using the algorithm describe above, the resulting matching scores are used to produce a list of  $m$  palmprint ( $m \ll M$ ) from the database, ranked from the best matching (with the highest matching score) to the worst (the lowest matching score).

During the evaluation process, each test image was used as input to the algorithm and matched against all 300 original images and the rank of the correct matching determined. This process was performed  $300 \times 300 = 90000$  times. Then, for each type of perturbations, the proportion of times during tests a correct matching appeared first (first rank recognition) is determined.

The percentage of correct identifications is reported as the correct (or Genuine) identification Rate (CIR): 96, 67% compared to Kumar's: GAR = 97.50% with EER = 3.03% at a specific threshold of 0.992.

Figure 6.5: The EER and ROC with threshold = 0.4



## 6.4 Evaluation of methods

The proposed algorithm is just applied on the entire palmprint due to the existing database. The results are not investigated with the part of palmprint and therefore, there is no estimation of scaling of the palmprint images in the pre-processing stage. What's more, there is no estimation of scaling

The programme can be used as an independent full product in order to insulate the image processing techniques as well as definitions mentioned in the previous chapter. A brief explanation of using input value and important image processing functions impacting on directly the accuracy and effectiveness of the proposed method are presents.

Moreover, programming is just used to demonstrate effectiveness and accuracy of proposed algorithm and thus the codes are not commented heavily. The proposed algorithm can be best developed by Matlab language – a high-level programming language containing hundreds of mathematical commands, equations, which is very useful in digital image processing. Therefore, the author wishes to study more deeply this language because of advantages in image processing algorithm programming (Gonzalez, 2008).

### 6.4.1 The factors impacting on the accuracy of the image normalizing

The following section presents the factors giving impact directly on the results of proposed algorithm. In the further work, these factors should be investigated to improve the accuracy of the matching stage.

First of all, many parameters are determines as constant value, thus the result is not always given best. For example, the grey level of image in processing converts a bitmap image to binary image is fixed instead of automatic threshold. In addition, the size of square in the function (Gozalez, 2008) identifying the boundary image is defined as constant parameter (4 pixels).

First of all, as mentioned in the previous chapters, in order to determine the boundary of the image, a threshold is used to convolve an input image binary image. Different grey level of the image returns different binary image, therefore different

boundary image. As an input file in function “im2bw”, “greyleveA.txt” file, a grey level table is defined as long as the boundary image returned has a shape of the hand. Actually, there is no demonstration whether this table will return the best binary image, which has effect on the demonstration of the proposed algorithm.

Secondly, in order to improve the estimation of translational displacement between images, the calculating of the phase of log-polar mapping images is very useful in term of theory. However, the accuracy is affected by the way how to determine the log-polar mapping of the images, which is not investigated in the project due to the limited time and word count. Actually, the log polar of the image was determined instead of polar of the image because most energy is concentrated in the low-frequency domain with natural images. In log-polar mapping, it is necessary to interpolate pixel intensity between discrete sample points. The accuracy of this interpolation has a significant impact on the total accuracy of image normalizing.

In addition, the original method of angle estimation in the proposed algorithm is from the algorithm for fingerprint recognition, and thus it is simple and effective to determine the rotation angle by finding the best phase between the Hanning images of the registered image and the testing image. However, there is really no demonstration about estimation of translational displacement.

What’s more, there is no investigation of determining the ROI of the proposed algorithm using the area between the middle and ring finger conversely with Zhang’s algorithm.

Although the preparation of Hanning window images and log-polar mapping is very useful to reduce the computational time, the input values is limited by the choosing the range of rotation angle from -10 to 10 degree. The preprocessing is not useful in case the rotation angle is out the above ranger. Therefore, it wastes computer memory.

The product is used to test the effectiveness of the proposed method, it is not commented heavily. In order to reduce computational time, the results of evaluation and the output values are saved in advance. Programming is not concentrated on building a software product, therefore, design diagrams are not provided completely.

Appendix C shows these codes in detail.

## 6.5 Evaluation of aims and objectives

### 6.5.1 Aims

Broadly speaking, the project has achieved its aims and objectives. Much effort has been invested in the literature research and findings support both the method employed and the evaluation of results obtained. The ROI was determined and applied to prepare the database for image matching. A palmprint recognition algorithm was proposed by modifying Phase-Only Correlation. This method was evaluated with the PolyU database. The effectiveness and accuracy of the modified algorithm was compared with Zhang's and Kumar's. However, the comparison between the proposed algorithms with the similar algorithm was not achieved completely, which are algorithms using the same Phase-Only Correlation.

### 6.5.2 Objectives

The experimental algorithm proposed has been successfully implemented. However, the precise objectives that have been met throughout the research course have been bent somewhat to satisfy a scope that has evolved with the deeper understanding of image processing. Firstly, the investigation of two existing recognition algorithms, Zhang's and Kumar's, were not really achieved. This objective just was presented as a discussion. Secondly, an application was developed in Matlab programming to demonstrate the effectiveness and usefulness of the proposed algorithm, but not existing other ones, although it was the useful toolkit for learning the basics of palmprint recognition algorithms based on Phase-Only Correlation.

# 7 Chapter 7: Conclusions and Recommendations

## 7.1 Conclusions

This project has presented a modified algorithm for the automatic matching of palmprint images using the Phase-Only Correlation method. The algorithm is based on a combination a few ideas including ROI extraction of Zhang's Algorithm, BLPOC from Takita's method and the estimation of rotation angle and translational displacement of Ito's method. For the new ROI's extraction, Zhang's method was modified by considering and computing the area between the ring finger and the middle finger instead of determining two other areas among fingers. To normalise palmprint images, the method of determining the angle of rotation for fingerprint is used as a preprocessing of the proposed algorithm. Finally, in order to improve a high accuracy of matching, Hanning window, a Gaussian Smoothing and a log-polar mapping are calculated and applied carefully to database the PolyU database used. The results of evaluation show that this project has achieved its aims and objectives with EER= 2,1%, threshold = 0.4, GAR = 98% and CIR =96,67%,

## 7.2 Further work

The following section present further works, which improve the effectiveness of the proposed algorithm and thus make it more applicable in access control/security systems.

The estimation of rotation angle and translational displacement should be investigated for image registration.

It is possible to improve the way for normalizing palmprint image before extracting ROI:

- + In the preprocessing stage, the estimation of rotation and translation will be investigated. The estimation of rotation angle can be used 1D POC instead of 2D. The proposed block matching may be useful in improving the accuracy of the method. In addition, because the analytical function fitting technique for correlation peak

estimation is essential, this method requires an iteration computation for nonlinear function fitting, resulting in significant increase in computation times. Addressing this problem, Nagashami et al (2006) proposed a peak evaluation formula (PEF) that directly estimates the POC peak location from actual 2D data array of the POC function. The use of peak evaluation formula is possible to eliminate iterative computation in the peak estimation.

- + The input value of functions is identified automatic.

- The proposed algorithm will find the scaling parameter in case that the testing image is the part of the palmprint.

- Finally, the proposed should be evaluated and compared against the others algorithm also using Phase-Only Correlation such as Ito's algorithm and Takita's algorithm,

# Bibliography

- Bouridane, A. (2009) *Imaging for forensic and security: From theory to practice*. London: Springer.
- Dai, J. and Z., J. (2010) 'Multi-feature based high-resolution palmprint recognition', *IEEE Trans. Pattern Analysis and Machine Intelligence*, PP (99), p. 1.
- Daku, B. L. F. (2006) *Matlab Tutor CD: Learning Matlab superfast*. Hoboken: John Wiley & Sons.
- Daugman, J. G. (1993) 'High Confidence Visual Recognition of Persons by a Test of Statistical Independence', *IEEE Trans. Pattern Analysis and Machine Intelligence*, 15 (11), pp. 1148-1161.
- Duta, N., Jain, A. K. and Mardia, K. V. (2001) 'Matching of Palmprint', *Pattern Recognition Letters*, 23 (4), pp. 477-485.
- Gonzalez, R. C. and Woods, R. E. (2008) *Digital image processing*. 3rd edn. New Jersey: Pearson Education.
- Gonzalez, R. C., Woods, R. E. and Eddins, S. L. (2004) *Digital Image Processing Using MATLAB*. London: Pearson Education.
- Gueham, M., Bouridane, A. and Crookes, D. (2007) 'Automatic recognition of partial shoeprints based on phase only correlation', *IEEE Trans. Image Processing*, 4 (4), pp. 441-444.
- Han, C. C., Cheng, H. L., Fan, K. C. and Lin, C. L. (2003) 'Personal Authentication Using Palmprint Features', *SCiVerse. Pattern Recognition*, 36 (2), pp. 371-381.
- Ito, K., Nakajima, H., Kobayashi, K., Aoki, T. and Higuchi, T. (2004) 'A fingerprint matching algorithm using phase-Only Correlation', *IEICE Trans. Fundamentals*, E87-A (3), pp. 682-691.
- Ito, K., Aoki, T., Nakajima, H. Kobayashi, K. and Higuchi, T. (2006) 'A palmprint recognition algorithm using phase-based image matching', *ICIP*, pp. 2669-2672.
- Ito, K., Iitsuka, S. and Aoki, T. (2009) 'A palmprint recognition algorithm using phase-based correspondence matching', *IEEE Trans. Image Processing*, pp. 1977-1980.
- Jain, A., Bolle, R. and Pankanti, S. (1999) *Biometrics: Personal Identification in Networked Society*. Boston: Kluwer Academic.
- Jain, A., Prabhakar, K. S., Hong, L. and Pankanti, S. (2000) 'Filterbank- Based Fingerprint Matching', *IEEE Trans. Image Processing*, 9 (5), pp. 846-859.
- Jain, A. K., Hong, L. and Bolle, R. (1997) 'On-Line Fingerprint Verification', *IEEE Trans. Pattern Analysis and Machine Intelligence*, 19 (4), pp. 302-314.
- Kumar, A. and S., H. C. (2004) 'Palmprint identification using palmcodes', *IEEE Trans. Image and Graphics*, p. 258.



- Laadjel M., K. F., Bouridane, A. and Boussakta, S. (2009) 'Degraded partial palmprint recognition for forensic investigations', *IEEE Trans. Image Processing*, pp. 1513-1516.
- Li, W., Zhang, D. and Xu, Z. (2002) 'Palmprint Identification by Fourier Transform', *Pattern Recognition and Artificial Intelligence*, 16 (4), pp. 417-432.
- Liu, C. J. and W., H. (2001) 'A Shape- and Texture-Based Enhanced Fisher Classifier for Face Recognition', *IEEE Trans. Image Processing*, 10 (4), pp. 598-608.
- Nagashima, S. (2006) 'A subpixel image matching technique using Phase-Only Correlation', *IEEE Trans. Intelligent Signal Processing and Communications*, p. 701.
- Nagashima, S., Ito, K., Aoki, T., Ishii, H. and Kobayashi, K. (2007) 'High-accuracy estimation of Image rotation using 1D phase Only Correlation', *IEICE Trans. Fundamentals*, E92A (1), pp. 235-243.
- Otsu, N. (1979) 'A Threshold Selection Method from Gray-Level Histograms', *IEEE Trans. Systems, Man, and Cybernetics*, 9 (1), pp. 62-66.
- Petrou, M. and B., P. (1999) *Image processing: the fundamentals*. New York: John Wiley & Sons.
- Reillo, R. S., C., Avilla, S. and Gonzalez, A. M. (2000) 'Biometric Identification through Hand Geometry Measurements', *IEEE Trans. Pattern Analysis and Machine Intelligence*, 22 (10), pp. 1168-1171.
- Russ, J. C. (1999) *The image processing handbook*. 5th edn. Chichester: CRC press LLC.
- Shu, W., Rong, G., Bain, Z. and Zhang, D. (2001) 'Automatic Palmprint Verification', *Int.J.Image and Graphics*, 1 (1), pp. 135-151.
- Shu, W. and D. Z., D. (1998) 'Automated Personal Identification by Palmprint', *Optical Eng.*, 37 (8), pp. 2659-2362.
- Takita, K., Aoki, T., Sasaki, Y., Higuchi, T. and Kobayashi, K. (2003) 'High accuracy subpixel image registration based on Phase only Correlation', *IEICE trans. Digital Signal Processing*, E86-A (8), pp. 1925-1934.
- Tsai, D. M. and C., C. H. (2002) 'Rotation-invariant pattern matching using wavelet decomposition', *IEEE Trans. Image Processing*, (23), pp. 191-201.
- Wildes, R. P. (1997) 'Iris Recognition: An Emerging Biometric Technology', *Proc. IEEE*, 85 (9), pp. 1348-1363.
- Wu, P. S. and L., M. (1997) 'Pyramid Edge Detection Based on Stack Filter', *ACM. Pattern Recognition Letters*, 18 (3), pp. 239-248.
- You, J., Li, W. and Zhang, D. (2002) 'Hierarchical Palmprint Identification via Multiple Feature Extraction', *Pattern Recognition and Artificial Intelligence*, 35 (4), pp. 847-859.
- Zhang, D. (2004) *Palmprint Authentication*. New York: Kluwer Academic.
- Zhang, D. (2000) *Automated Biometrics-Technologies and Systems*. New York: Kluwer Academic.

Zhang, D. and S., W. (1999) 'Two Novel Characteristics in Palmprint Verification: Datum Point Invariance and Line Feature Matching', *SciVerse.Pattern Recognition*, 32 (4), pp. 691-702.

<http://blinkdagger.com/matlab/matlab-introductory-fft-tutorial/>

<http://www.printrakinternational.com/omnitrak.htm>—Printrak Automatic Palmprint Identification System, 2003

[http://ieeexplore.ieee.org/search/srchabstract.jsp?tp=&arnumber=5557887&queryText%3Dfeature+based+recognition+palmprint%26openedRefinements%3D\\*%26searchField%3DSearch+All](http://ieeexplore.ieee.org/search/srchabstract.jsp?tp=&arnumber=5557887&queryText%3Dfeature+based+recognition+palmprint%26openedRefinements%3D*%26searchField%3DSearch+All)

[http://www.sciencedirect.com/science?\\_ob=ArticleURL&\\_udi=B6V15-3SNV2KY-3&\\_user=122879&\\_coverDate=03%2F31%2F1997&\\_rdoc=1&\\_fmt=high&\\_orig=search&\\_origin=search&\\_sort=d&\\_docanchor=&view=c&\\_searchStrId=1465680284&\\_rurunOrigin=scholar.google&\\_acct=C000010138&\\_version=1&\\_urlVersion=0&\\_userid=122879&md5=650800d5dcc02414389a3db61193b009&searchtype=a](http://www.sciencedirect.com/science?_ob=ArticleURL&_udi=B6V15-3SNV2KY-3&_user=122879&_coverDate=03%2F31%2F1997&_rdoc=1&_fmt=high&_orig=search&_origin=search&_sort=d&_docanchor=&view=c&_searchStrId=1465680284&_rurunOrigin=scholar.google&_acct=C000010138&_version=1&_urlVersion=0&_userid=122879&md5=650800d5dcc02414389a3db61193b009&searchtype=a)

[http://svnnext.it-sudparis.eu/svnview2-eph/ref\\_syst/Tools/PerformanceEvaluation/doc/howTo.pdf](http://svnnext.it-sudparis.eu/svnview2-eph/ref_syst/Tools/PerformanceEvaluation/doc/howTo.pdf)

[http://books.google.com.vn/books?id=B2UTolEQbyoC&pg=PA210&lpg=PA210&dq=estimate+rotation+angle+using+POC&source=bl&ots=VWew2pUkqr&sig=PSsLLu5C0LX9Z6d5On0kQgf\\_WkE&hl=vi&ei=FD51TPjrOlajAfc1LidBg&sa=X&oi=book\\_result&ct=result&resnum=3&ved=0CCMQ6AEwAg#v=onepage&q=estimate%20rotation%20angle%20using%20POC&f=false](http://books.google.com.vn/books?id=B2UTolEQbyoC&pg=PA210&lpg=PA210&dq=estimate+rotation+angle+using+POC&source=bl&ots=VWew2pUkqr&sig=PSsLLu5C0LX9Z6d5On0kQgf_WkE&hl=vi&ei=FD51TPjrOlajAfc1LidBg&sa=X&oi=book_result&ct=result&resnum=3&ved=0CCMQ6AEwAg#v=onepage&q=estimate%20rotation%20angle%20using%20POC&f=false)

[http://books.google.com.vn/books?id=B2UTolEQbyoC&pg=PA210&lpg=PA210&dq=A+high-accuracy+rotation+estimation+algorithm+based+on+1D+phase+Only+Correlation&source=bl&ots=VWfx4m-pox&sig=2-dKPXp61HijgIkaJiNUB7qb-Xc&hl=vi&ei=I8wfTeHGL8G3hQe1mai3Dg&sa=X&oi=book\\_result&ct=result&resnum=2&ved=0CB0Q6AEwAQ#v=onepage&q=A%20high-accuracy%20rotation%20estimation%20algorithm%20based%20on%201D%20phase%20Only%20Correlation&f=false](http://books.google.com.vn/books?id=B2UTolEQbyoC&pg=PA210&lpg=PA210&dq=A+high-accuracy+rotation+estimation+algorithm+based+on+1D+phase+Only+Correlation&source=bl&ots=VWfx4m-pox&sig=2-dKPXp61HijgIkaJiNUB7qb-Xc&hl=vi&ei=I8wfTeHGL8G3hQe1mai3Dg&sa=X&oi=book_result&ct=result&resnum=2&ved=0CB0Q6AEwAQ#v=onepage&q=A%20high-accuracy%20rotation%20estimation%20algorithm%20based%20on%201D%20phase%20Only%20Correlation&f=false)

<http://www.mathworks.com>

[http://support.bioid.com/sdk/docs/About\\_EER.htm](http://support.bioid.com/sdk/docs/About_EER.htm)

## Appendix A. Figures and diagrams

Figure 1.1 : Palmprint feature definition principal lines and wrinkles(Internet source).

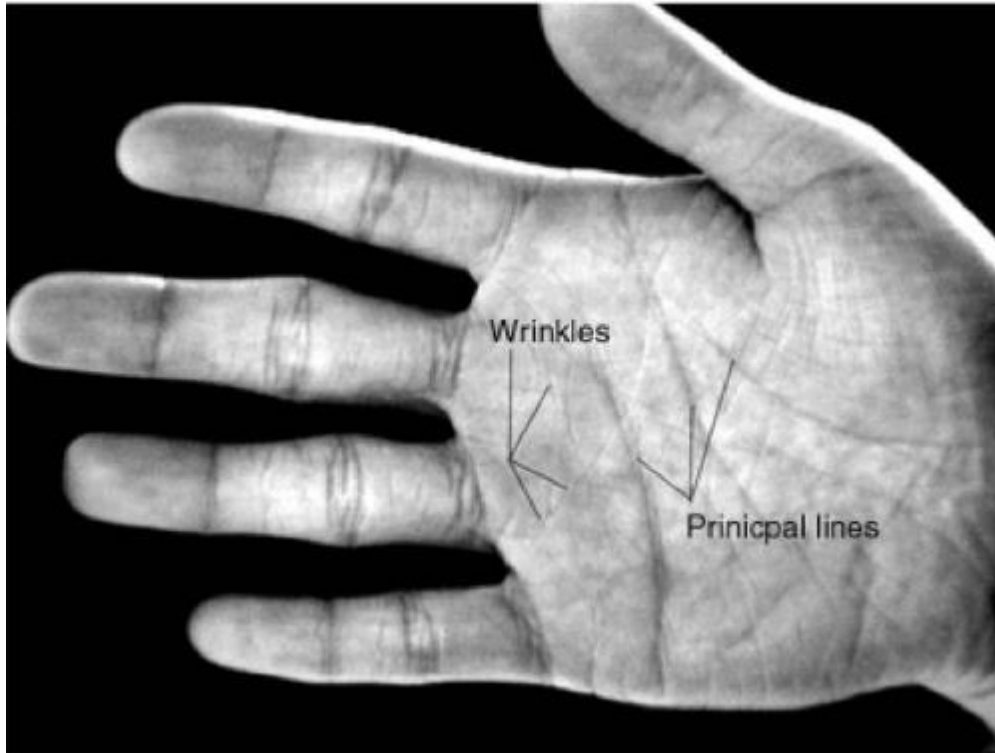


**Figure 2.1: When two image are similar and dissimilar, comparison between POC and original correlation (Internet source).**

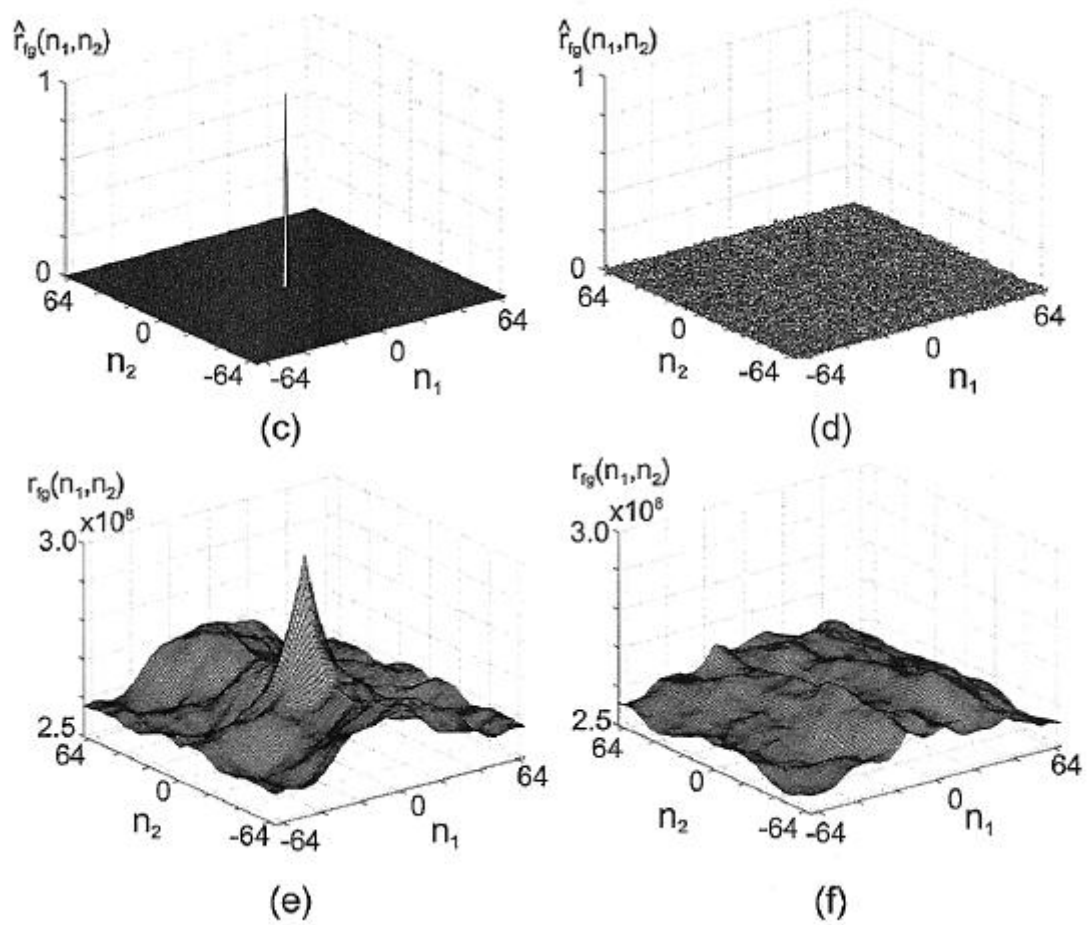


**Figure 2.2: Comparison between POC and BLPOC (Ito,2006)**

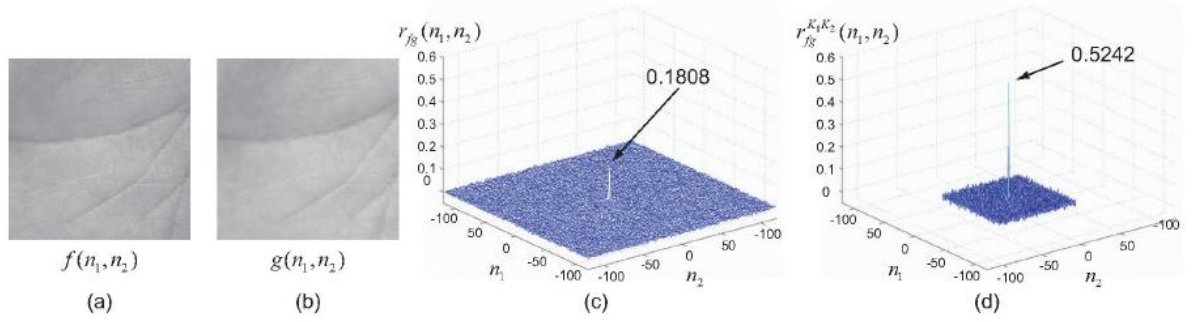


Fig. 1. Example of genuine matching using the original POC function and the BLPOC function: (a) registered palmprint image  $f(n_1, n_2)$ , (b) input palmprint image  $g(n_1, n_2)$ , (c) original POC function  $r_{fg}(n_1, n_2)$  and (d) BLPOC function  $r_{fg}^{K_1K_2}(n_1, n_2)$  with  $K_1/M_1 = 0.40$  and  $K_2/M_2 = 0.40$ .

**Figure 3.1: the procedure of PalmCode of Kuma(2004)**

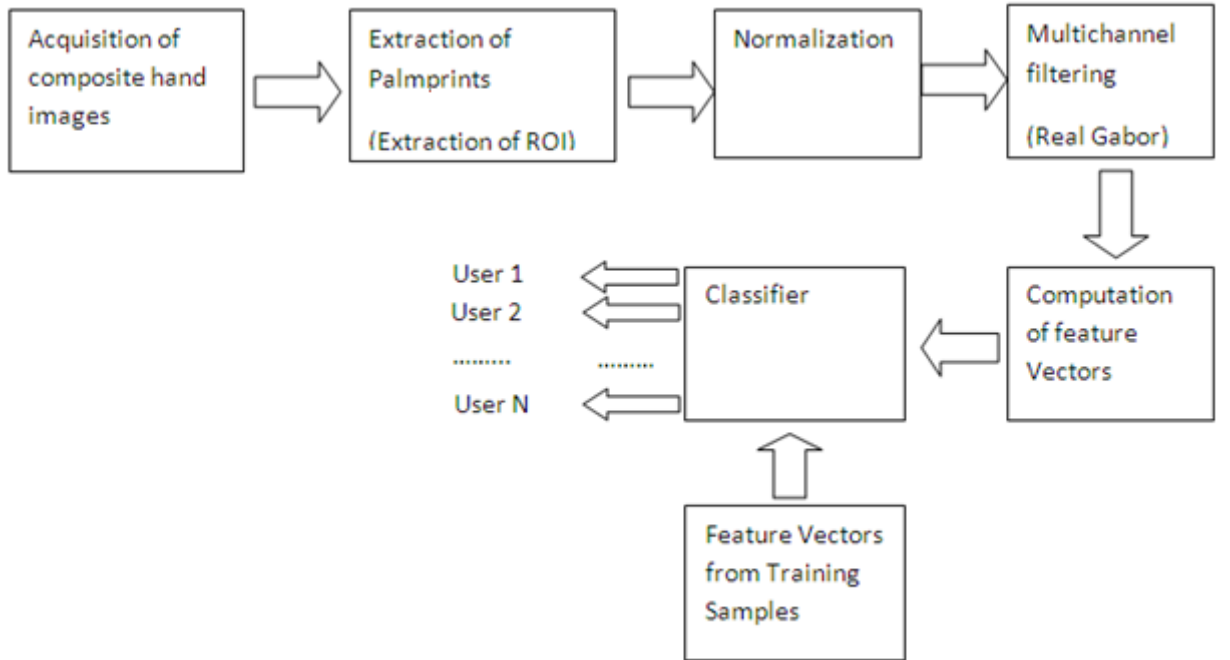


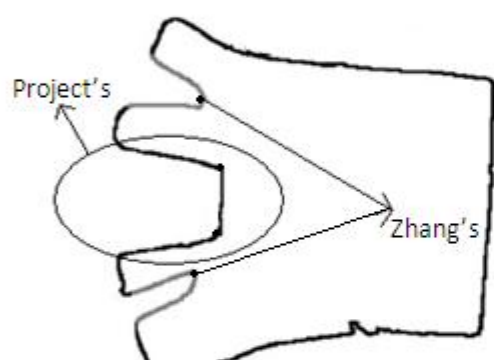
Figure 3.2: Comparison of Extracting ROI between Zhang's and project's



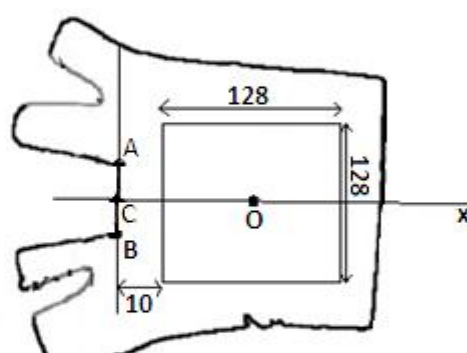
(a)



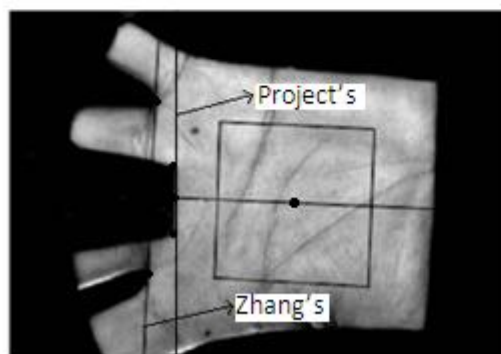
(b)



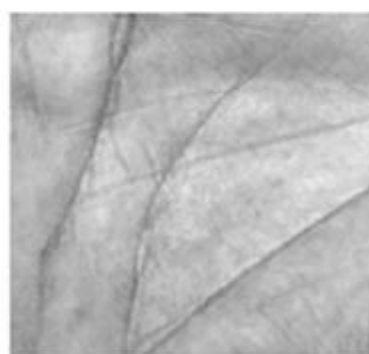
(c)



(d)



(e)



(f)

**Figure 4.1: Hanning Image**



**Figure 4.2: Period of DFT**

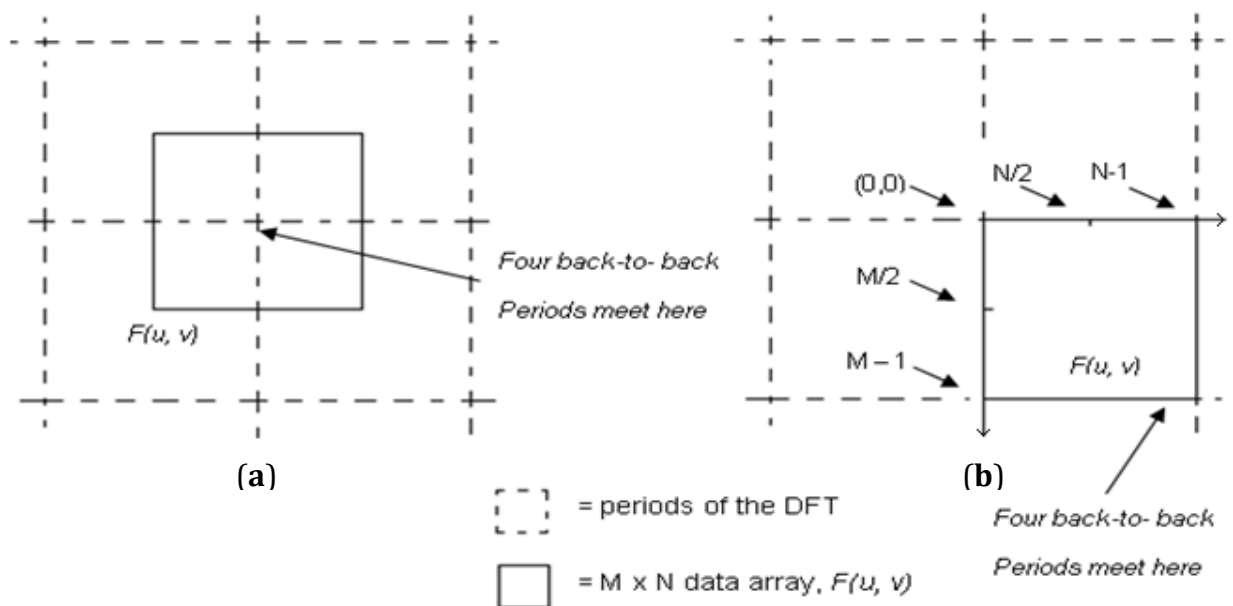
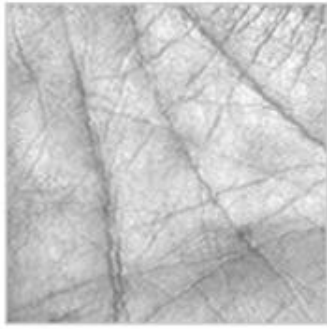
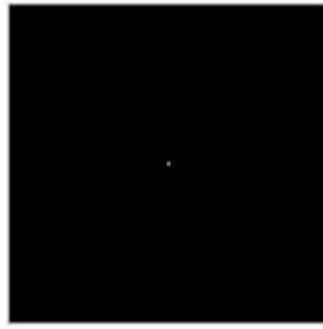


**Figure 4.** (a): A 2-D DFT showing an infinite number of periods. The solid area is the  $M \times N$  data array,  $F(u, v)$ . This array consists of four quarters periods; (b): A shifted DFT obtained by multiplying  $f(x, y)$  by  $(-1)^{x+y}$  before computing computing  $F(u, v)$ . The data contains one complete, centered period.

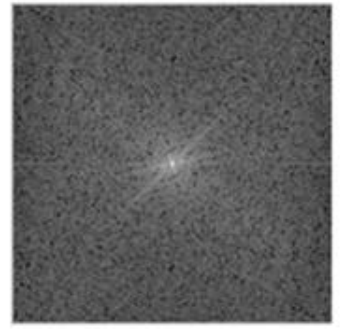
**Figure 4.3 Display of DFT**



(a)



(b)



(c)

*(a) An image of ROI of a palmprint; (b) display of  $|F(u,v)|$ ; (c) display of  $\log[1+|F(u,v)|]$*



**Figure 5.1 the centre of gravity of the image.**

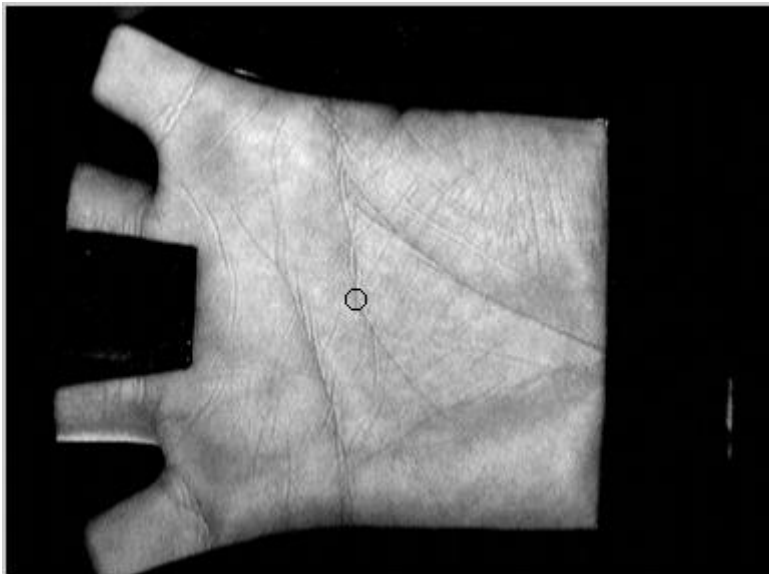


**Figure 5.2 Amplitude spectrum**

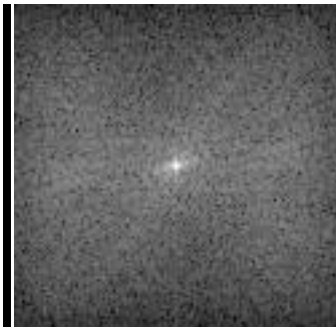


**Figure 5.3 Log-Polar Mapping Image**

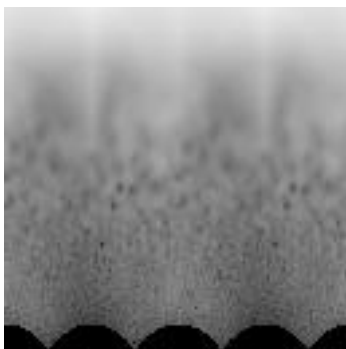


**Figure 5.4 Preprocessing of proposed method**

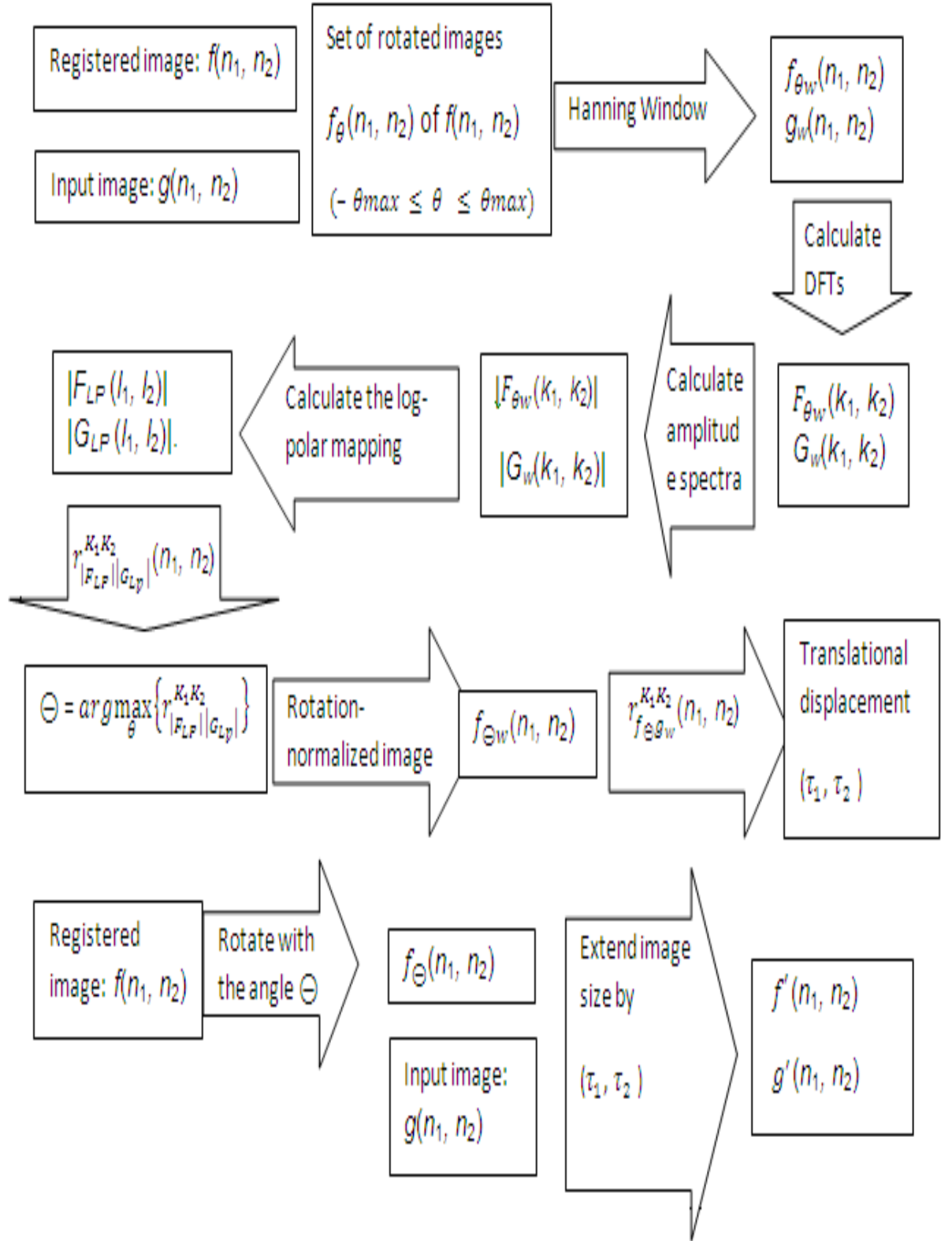
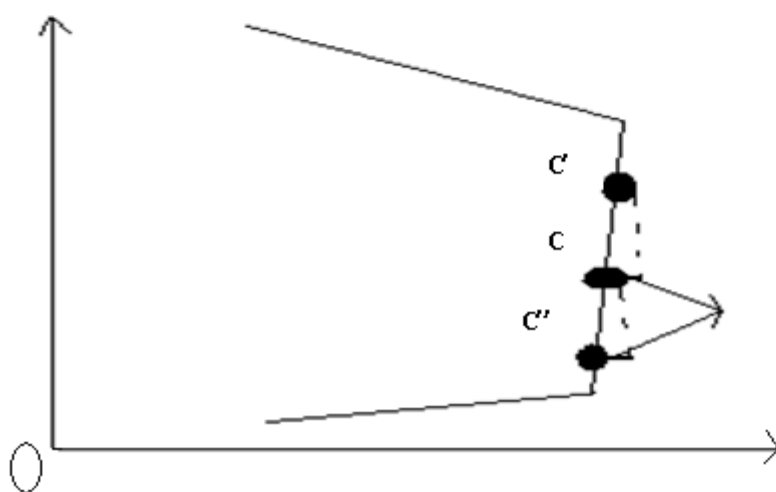
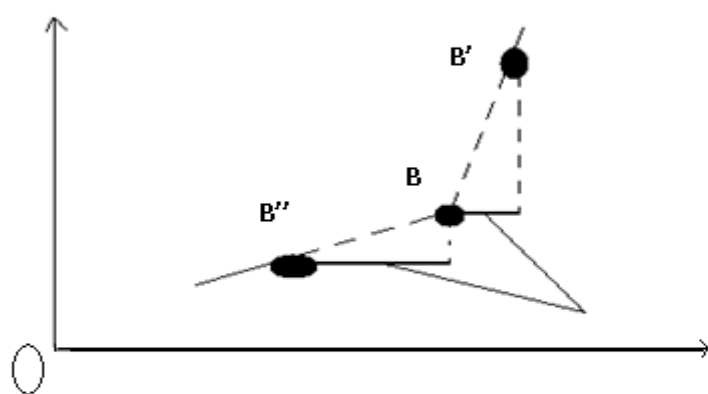
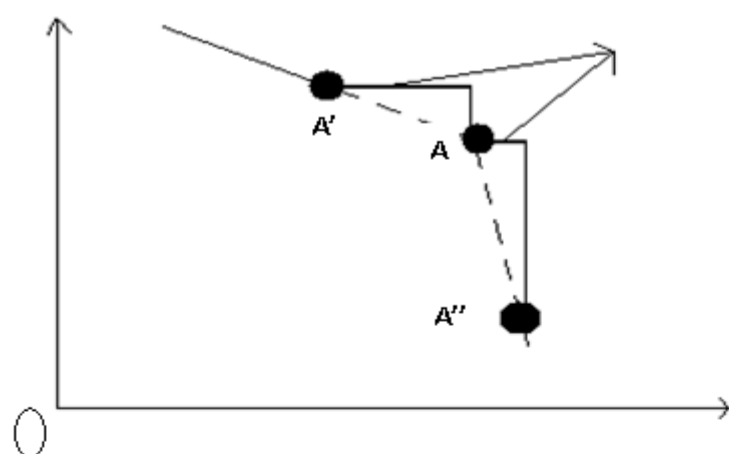
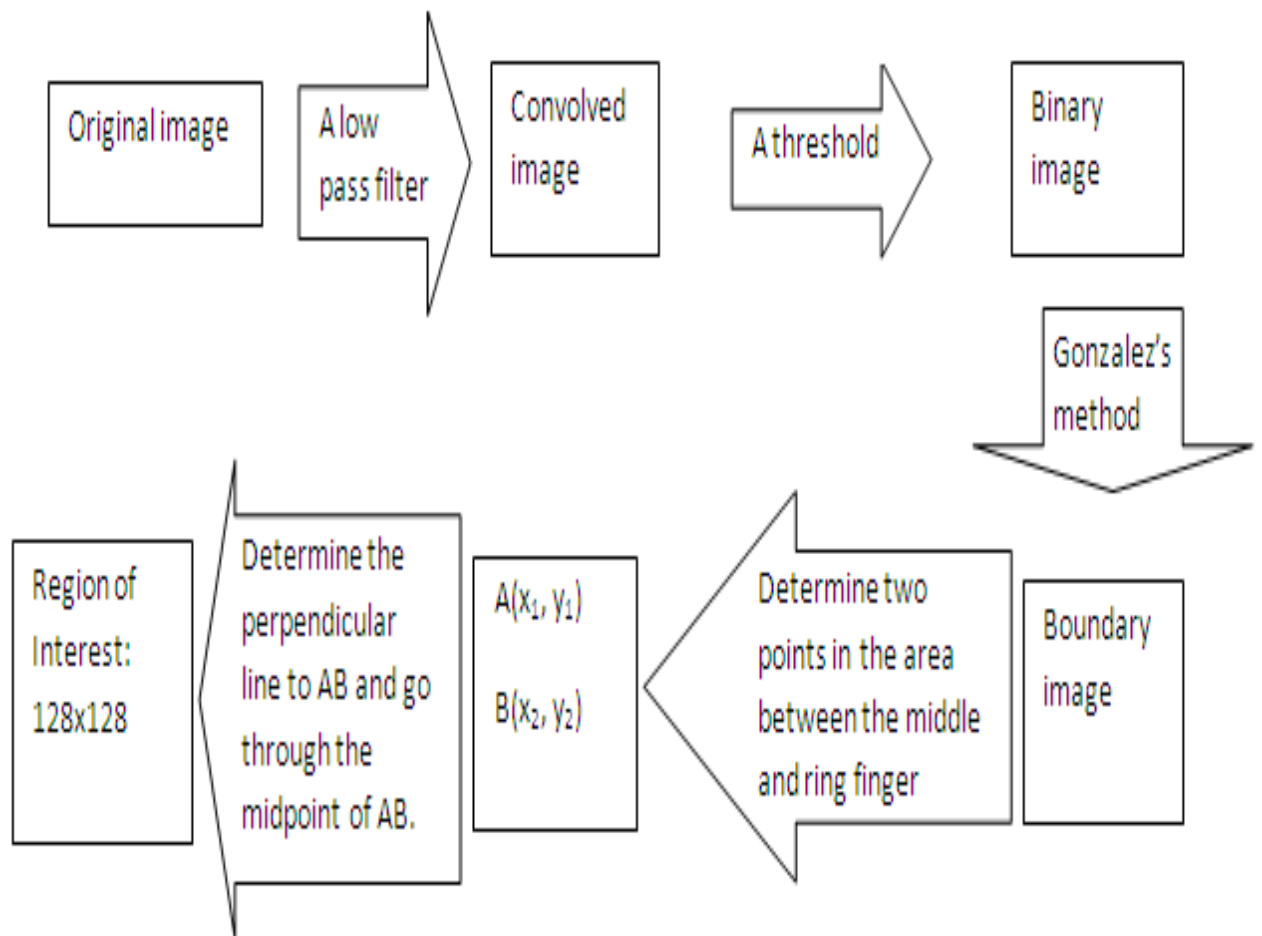


Figure 5.5: How to find the place of A and B points



**Figure 5.6 The Procedure to extract Region of Interest.**



**Figure 5.7: Matching stages**

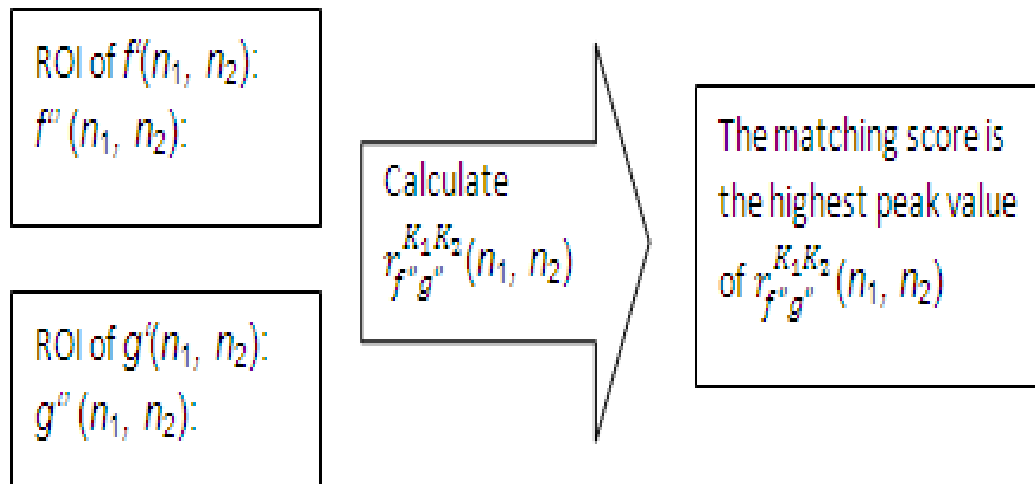


**Figure 6.1: FRR, FAR and Threshold(Internet source)**

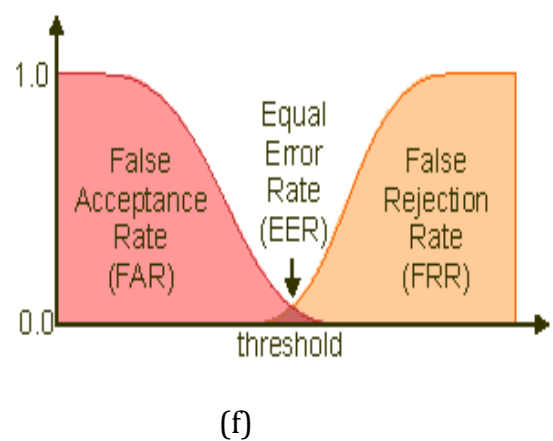
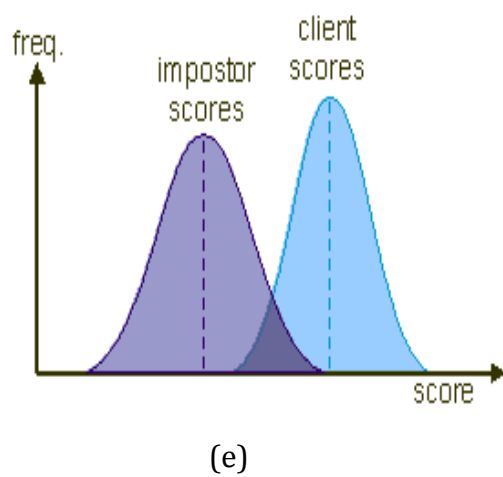
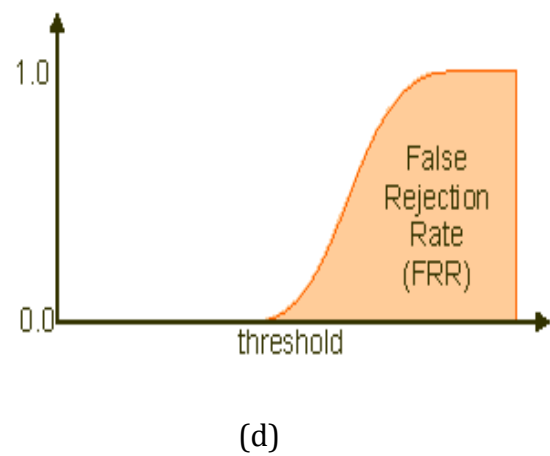
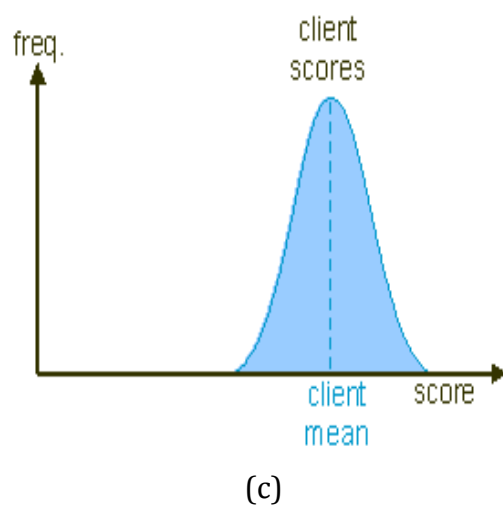
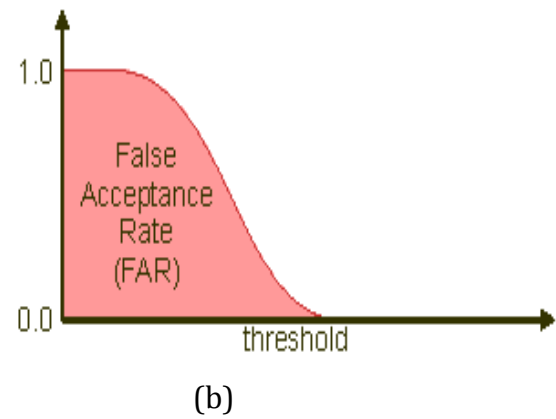
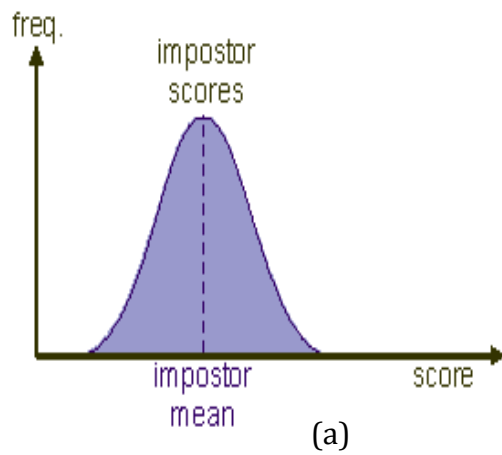


**Figure 6.2 A sample of Palmprint image in PolyU database**

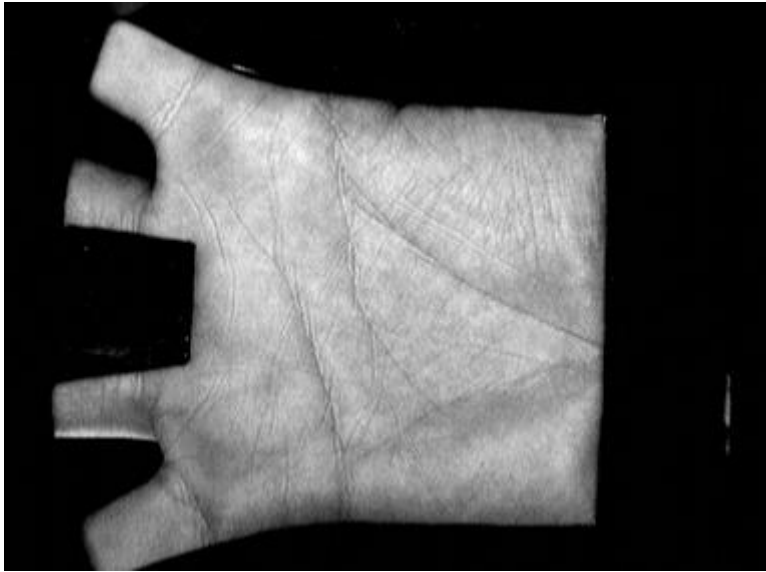
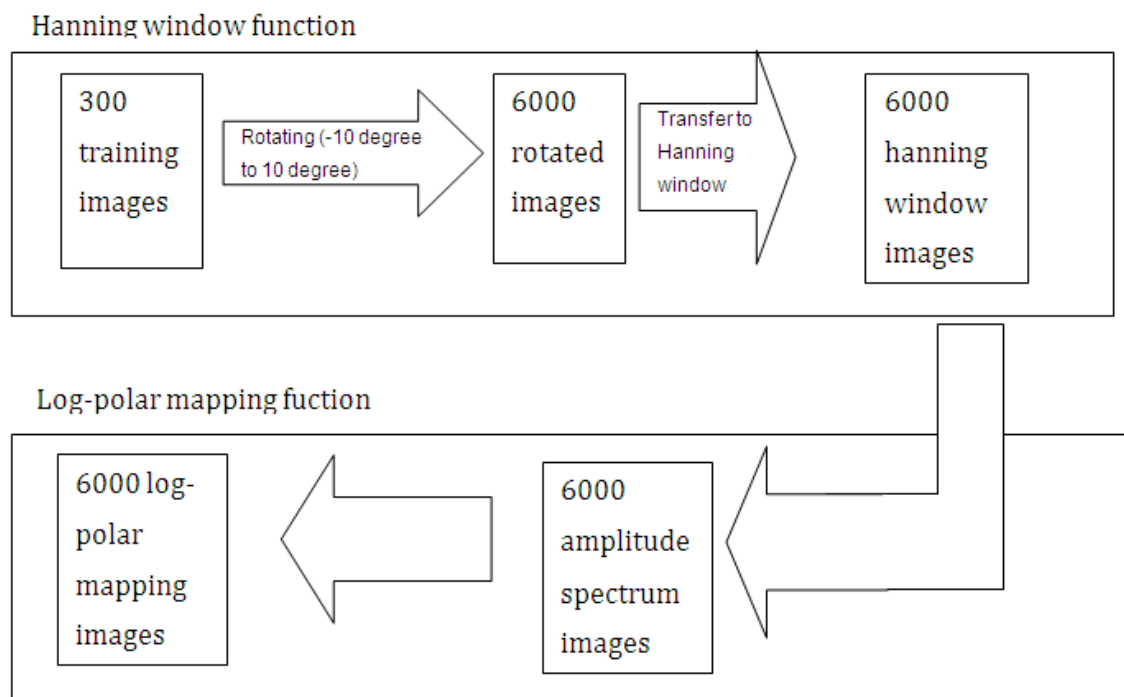


**Figure 6.3: Preparation of database**





## **Appendix B. Terms of reference**

### **CG174 MSc Computing Project Terms of Reference**

1) Project Title: A modified Phase Only Correlation for Palmprint Recognition

2) Student: Nguyen Thi Thuy Duong

3) Supervisor: Prof Ahmed Bouridane

4) TOR Reviewer: Dr Joe Faith

5) Background (outline):

a. What you intend to do

- Investigate a modified phase only correlation methods for use in Palmprint Recognition. In addition, I will also investigate and propose an efficient Region of Interest (ROI) extraction to further improve the recognition rates.
- Develop a Graphical demonstrator using MATLAB programming language to show the operations of such system
- Carry out extensive experiments using the Hong Kong Palmprint (PolyU) palmprint database to demonstrate the findings
- Analyse and assess the performances of the recognition including a comparative study against the system proposed by Zhang et al.

b. Why you intend to do:

- The rapid growth of e-commerce applications requires reliable and automatic personal identification for effective security access/control. While traditional, automatic, personal identification approaches have some limitations such as a physical key, an ID card, and a passport stolen or lost; a password guessed or forgotten, Biometric personal identification is emerging as a powerful means for automatically recognizing a person's identity (Zhang, 2003).
- Among many biometric techniques, palmprint recognition is one of the most reliable approaches, since a palmprint has a large inner surface of the hand

containing many features such as principle lines, ridges, minutiae points, singular points and texture(Ito, 2006). Compared with other biometric traits, the advantages of palmprint are the availability of large palm area for feature extraction, the simplicity of data collection and high user acceptability (Laadjel, 2008).

- (Kumar, 2004) also stated that a palmprint image can be analyzed as texture, which is random rather than uniform. Any commercial development of an automated palmprint based identification system would require automated extraction of region of interest i.e. palmprint area, while ignoring fingers, wrist, and background (if any).

- A major approach for palmprint recognition today is to extract feature vectors corresponding to individual palmprint images and to perform palmprint matching based on some distance metric (Ito, 2006).

- One of the most difficult problems of palmprint recognition is that the matching performance is significantly influenced by many parameters at the feature extraction process, which may vary depending on environmental factors of palmprint image acquisition. The reliability on the performance of a personal recognition system largely depends on its degree of tolerance due to rotation, translation, and scaling distortions (Kumar, 2004).

- (Fortunately), however, Phase Only Correlation (POC) has some remarkable properties such as invariance to image translation, invariance to illumination changes, and immunity against additional noise (Laadjel, 2009). The technique can be successfully applied to fingerprint recognition, iris recognition and shoeprint recognition.

c. What methodology you will use:

The structured approach also known as quantitative research is used to achieve the required results, including:

Eight objectives are presented in the next section.

Design: an existing palmprint database, a proposed algorithm, a system written in MATLAB and the comparison of results between the proposed algorithm and some existing or similar ones for the purpose of assessing the performances.

Sample: Using Zhang's algorithm (2003) and applying some image processing, a new palmprint image database are created from PolyU.

## 5.1 Recognition/Verification/Watch-list

It is commonly known that a typical biometric recognition scenario, as all biometric applications, can be classified into one of two types: verification (or authentication) and identification (or recognition). In some applications, a third scenario may be added. For example, Phillips et al. in the Face Recognition Vendor Test (FRVT) [9] define another type and is called the "Watch-list".

### 5.1.1 Verification: Am I who I claim to be?

This scenario can be employed in a control access point application. It is used when a subject provides an alleged identity. The system then performs a one-to-one match that compares a query biometric image against the template image, of the person whose identity is being claimed, stored in the database. If a match is made, the identity of the person is verified.

In other words, the verification test is conducted by dividing the subjects into two groups:

Clients: people trying to gain access using their own identity.

Imposters: people trying to gain access using a false identity, i.e. an identity known to the system but not belonging to them.

The percentage of imposters gaining access and clients rejected access are reported as the False Acceptance Rate (FAR) and the False Rejection Rate (FRR).

### 5.1.2 Recognition: Who am I?

This mode is used when the identity of the individual is not known in advance. The entire template database is then searched for a match to the individual concerned in a one-to-many search. If a match is made the individual is identified.

The recognition test works from the assumption that all biometric images being tested are of known persons. The percentage of correct identifications is reported as

the Correct (or Genuine) Identification Rate (CIR) or the percentage of false identifications is reported as the False Identification Rate (FIR).

#### 6) The Aims of the project:

Research question: How can improve palmprint recognition using POC method?

To determine the area of palmprint and applying some image processing techniques to them (Region of Interest Extraction).

To modify Phase-only Correlation to improve palmprint recognition.

To evaluate the proposed algorithm and compare it to some existing and similar ones

#### 7) Objectives:

To complete a literature search and literature of palmprint recognition techniques in commercial application.

To develop and evaluate some effective algorithms based on Phase-only Correlation for image recognition, particular shoeprint, fingerprint, iris and palmprint.

To investigate some existing palmprint recognition algorithms using different techniques

To apply some image processing techniques to palmprint image database and determine the region of interest for creating a new database.

To identify and gather the most sufficient palmprint recognition technique for Region of Interest Extraction

To modify an existing algorithm to improve palmprint recognition using Phase-only Correlation.

To develop an application in MATLAB programming language to demonstrate the usefulness of proposed algorithm and some existing other ones.

To evaluate the result of the proposed algorithm and compare it against other ones.

#### 8) Dissertation Outline:

Title page: Will be layout as the specimen sheet that was provided to me by the university.

Authorship Declaration: This will be a statement sign by me certifying that the report and the work described in are my own.

Acknowledgements: Here I will acknowledge help given to me either from people outside the department, my supervisor or from staff inside the department other than the supervisor.

Abstract: Here I will have a brief description of the work contained in the report.

List of Contents: Here I will have the list of contents of the report by chapter and sub-section against page numbers.

Main Body:

Introduction:

Here I will describe the background to the project, give a clear statement of the aims and objectives, provide an overview of the work done and my principal conclusions. I will use the term of reference document to form the basis for the introduction

Literature Review:

This section will cover the background of the project by critically discussing relevant papers which will help to understand the aims of the project that leads to the hypothesis question. This section will be divided into 3 chapters. The 3 chapters are:

Chapter 1. To complete a literature search and literature of palmprint recognition techniques in commercial application.

Chapter 2. To collect and evaluate some effective algorithms based on Phase-only Correlation for image recognition, particular shoeprint, fingerprint, iris and palmprint.

Chapter 3. To investigate some existing palmprint recognition algorithms using other different techniques

b. Practical work:

This section will focus of what experiments I design to test the Question that I proposed. This section will have 3 chapters:

Chapter 4. To apply some image processing techniques to palmprint image database and determine the region of interest for creating a new database.

The last section is to identify and gather the most sufficient palmprint recognition technique for Region of Interest Extraction.

Chapter 5. To modify an existing algorithm to improve palmprint recognition using Phase-only Correlation.

c. Hypothesis testing:

This section will cover the evaluation of the experiments that I designed and used and about the management and approach I used for this project.

Chapter 6. To evaluate the result of the proposed algorithm and compare it against other ones.

Chapter 7: Conclusions and recommendations:

This section is concerned with conclusions from the investigation including further works.

Reference:

Here I will use the Harvard system to write my reference list of all the quotes or paraphrasing that I will use during my report so that I will avoid any plagiarism.

Appendices:

Here I will have material that is not necessary to a first reading of the report and documentation about the product. Possible documentation is terms of reference, experiments specification, and results.

9) Relationship to the Course (Next meeting):

- Research method:

- Project management:

- System development:
- Database:
- Implementation of oriented-object language:

#### 10) Sources of information / Bibliography:

Gonzalez, R. C., and Woods, R. E. (2008) Digital image processing 3rd edn. Upper Saddle River, N.J. ; Harlow : Pearson Education.

Gueham, M., Bouridane, A. and Crookes, D. (2007) 'Automatic Recognition Of Partial Shoeprints Based on Phase-only Correlation', IEEE, 4, pp. 441-444 [Online]. Available at: <http://ieeexplore.ieee.org/> (Accessed: 13 March 2010).

Ito, K., Aoki, T., Nakajima, H., Kobayashi, K. and Higuchi, T. (2006) 'A Palmprint Recognition Algorithm Using Phase-based Image Matching', IEEE, pp. 2669-2672 [Online]. Available at: <http://ieeexplore.ieee.org/> (Accessed: 13 March 2010).

Kumar, A. and S., H. C. (2004) 'Palmprint Identification Using PalmCode', IEEE, pp. 258-261 [Online]. Available at: <http://ieeexplore.ieee.org/> (Accessed: 13 March 2010).

Laadjel, M., Bouridane, A. and Kurugollu, F. (2008) 'Eigenspectra Palmprint Recognition', IEEE, pp. 382-385 [Online]. Available at: <http://ieeexplore.ieee.org/> (Accessed: 13 March 2010).

Laadjel, M., Kurugollu, F., Bouridane, A. and Boussakta, S. (2009) 'Degraded Partial Palmprint Recognition For Forensic Investigation', IEEE, pp. 1973-1976 [Online]. Available at: <http://ieeexplore.ieee.org/> (Accessed: 13 March 2010).

Zhang, D., Wai-Kin Kong, You, J. and Wong, M. (2003) 'Online Palmprint Identification', IEEE, 25 (9), pp. 1041-1050 [Online]. Available at: <http://ieeexplore.ieee.org/> (Accessed: 13 March 2010).

Bibliography:

<http://www.mathworks.com/>

#### 11) Resources/Constraint:

The resources that I will use for the project are a PolyU database that I will acquire from Prof Ahmed Bouridane and will have Windows XP or Linux on it to carry out the experiments, my personal laptop to write the dissertation, the university printers to print out my work, two CDs and a two GB USB disk to store and back up my work. Furthermore, in order to illustrate these algorithms, I will use MATLAB language to design a system.

## 12) Schedule of Activities:



